Author's response

Study of the dependence of stratospheric ozone long-term trends on local solar time. Eliane Maillard Barras et al., Atmos. Chem. Phys. Discuss., https://doi.org/10.5194/acp-2020-101.

Dear Referees,
Dear Editor Jens-Uwe Grooß,

We would like to thank the referees for the detailed review of the manuscript and for their constructive and helpful comments and suggestions. We have taken the remarks into account and we are presenting the detailed answers in the following. We attach a revised version of the manuscript with marked changes.
We hope having satisfactorily addressed the suggestions and remarks.
The referee's comments are given in italic, our responses are given in blue, and the corresponding changes in the manuscript in grey.

Best regards,
Eliane Maillard Barras (on behalf of all co-authors)

Answers to Referee nr 1:

In view of some recent work showing unexpected negative ozone trend in the lower stratosphere in the NH, a critical survey of possible systematic effects in ozone datasets is highly demanded. Therefore, the paper presented by Barras et al. studying possible effects of LST when deriving trends from MWR observation is a timely contribution in this context.
The paper is generally well written and is presenting its results well organized. It compares the Payerne observations with other instruments in order to homogenize the dataset and takes extensively care to eliminate impacts of various technical changes of the instrument. It extends the analysis by comparing the results with model results which essentially support the conclusions of the authors.
The paper needs in my opinion only minor changes. Some comments below and in the attached pdf should give some suggestions how the paper can be improved.

Thank you very much for your positive feedback. We address in the following the comments below and the comments of the attached pdf file.

General remarks

The motivation of the paper (reliable ozone trends after 2000) should be presented clearer and much further at the beginning of the paper.

We modified the abstract for a clearer presentation of the motivation of the paper.

Reliable ozone trends after 2000 are essential to detect early ozone recovery. However, the long-term ground-based and satellite ozone profile trends reported in the literature show a high variability. The reason for variability in the reported long-term trends has multiple possibilities such as the measurement timing and the dataset quality.

The Payerne Switzerland microwave radiometer (MWR) ozone trends are significantly positive at 2 to 3 %/decade in the upper stratosphere (5--1 hPa, 35--48 km), with a high variation with altitude. This is in accordance with the northern hemisphere (NH) trends reported by other ground-based instruments in the

SPARC LOTUS project. In order to determine what part of the variability between different datasets comes from measurement timing, Payerne MWR and SOCOL v 3.0 chemistry-climate model (CCM) trends were estimated for each hour of the day with a multiple linear regression model. Trends were quantified as a function of local solar time (LST). In the mid- and upper stratosphere, differences as a function of LST are reported for both the MWR and simulated trends for the post-2000 period. However, these differences are not significant at the 95% confidence level. In the lower mesosphere (1--0.1 hPa, 48--65 km), the 2010-2018 day- and nighttime trends have been considered. Here again, the variation of the trend with LST is not significant at the 95% confidence level. Based on these results we conclude that significant trend differences between instruments cannot be attributed to a systematic temporal sampling effect.

The dataset quality is of primary importance in a reliable trend derivation and multi-instrument comparison analyses can be used to assess the long-term stability of data records by estimating the drift and bias of instruments. The Payerne MWR dataset has been homogenized to ensure a stable measurement contribution to the ozone profiles and to take into account the effects of three major instrument upgrades. At each instrument upgrades, a correction offset has been calculated using parallel measurements or simultaneous measurements by an independent instrument. At pressure levels smaller than 0.59 hPa (above ~50 km), the homogenization corrections to be applied to the Payerne MWR ozone profiles are dependent on local solar time (LST). Due to the lack of reference measurements with a comparable measurement contribution at a high time resolution, a comprehensive homogenization of the sub-daily ozone profiles was possible only for pressure levels larger than 0.59 hPa.

The ozone profile dataset from the Payerne MWR, Switzerland, was compared with profiles from the GROMOS MWR in Bern, Switzerland, satellite instruments (MLS, MIPAS, HALOE, SCHIAMACHY, GOMOS), and profiles simulated by the SOCOL v3.0 CCM. The long-term stability and mean biases of the time series were estimated as a function of the measurement time (day- and nighttime). The homogenized Payerne MWR ozone dataset agrees within +-5% with the MLS dataset over the 30 to 65 km altitude range and within +-10% of the HARMonized dataset of OZone profiles (HARMOZ, limb and occultation measurements from Envisat) over the 30 to 65 km altitude range. In the upper stratosphere, there is a large nighttime difference between Payerne MWR and other datasets, which is likely a result of the mesospheric signal aliasing with lower levels in the stratosphere due to a lower vertical resolution at that altitude. Hence, the induced bias at 55 km is considered an instrumental artefact and is not further analyzed.

The steps of the homogenization process should be summarized first, and the technical reasons what causes the differences should be shortly explained somewhat in addition.

The technical reasons for the differences are detailed in p5 lines136-138 and p6 lines 172-174. We added a short description of the homogenization steps in the abstract.

The Payerne MWR dataset has been homogenized to ensure a stable measurement contribution to the ozone profiles and to take into account the effects of three major instrument upgrades. At each instrument upgrades, a correction offset has been calculated using parallel measurements or simultaneous measurements by an independent instrument. At pressure levels smaller than 0.59 hPa (above ~50 km), the homogenization corrections to be applied to the Payerne MWR ozone profiles are dependent on local solar time (LST).

The homogenization is now described in a separate section (Section 3) from the datasets description as suggested by referee 2. We added also a summary of the homogenization process at the beginning of section 3 and shortly explain the technical reasons causing the differences.

The homogenization of the Payerne MWR dataset was performed in stages. First, the integration time has been adapted at each upgrade transition to ensure a constant measurement contribution over the dataset time range. At the spectrometer upgrade transition (AOS to FFTS), a correction offset has been

calculated over one year of simultaneous measurements. At the front-end and the Gunn oscillator upgrades transitions, the correction offsets have been calculated using simultaneous measurements by an independent instrument, resp. by the Bern MWR and by MLS satellite. Moreover, the homogenization corrections to be applied to the Payerne MWR ozone profiles are dependent on local solar time (LST).

From Fig. 3, the bias from the technical interventions is significant. The authors are asked to show the full (deseasonalized) timeseries with and without applying the corrections.

A figure has been added after Figure 3 presenting the full deseasonalized timeseries with and without applying the corrections.

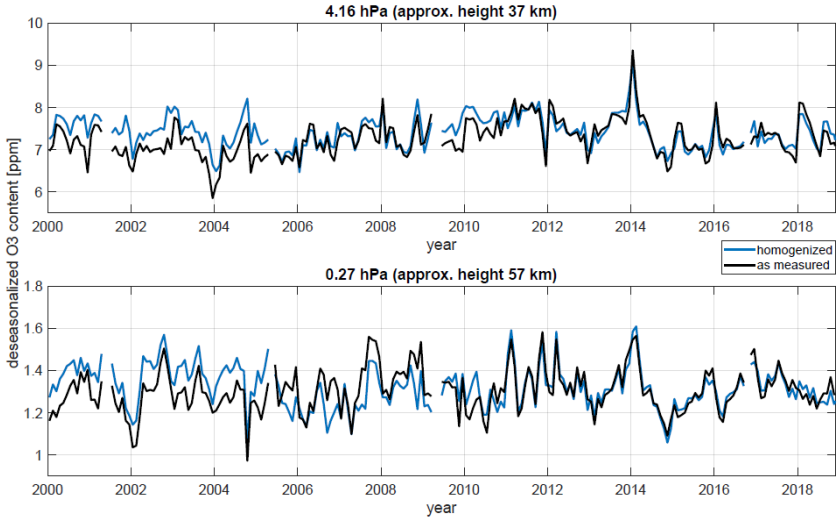

Figure 4. Deseasonalized ozone monthly means timeseries before (in black) and after (in blue) the homogenization for two representative layers in the middle stratosphere and in the low mesosphere.

The rational of the search for LST dependence of the O3 trend besides a more technical effect should be explained in the paper. As long as one is in a quasi linear domain, the LST should have only a small impact on the trend, I guess. This is what one can see in Para 4.2.3 Fig. 9 c).

The rational of the search for LST dependence is explained in the introduction section p3 line 65-74 and is modified in the updated version (new version p3 line 72-81).
We understand the « in a quasi linear domain » in the referee's comment as the O3 variation vs time. However, in the low mesosphere, the O3 content varies with time in a non linear way with O3 first decreasing with LST and then increasing again, while in the stratosphere, the O3 is maximal in the afternoon (as plotted in Fig 6 of the updated version).
The intercomparison of trends derived from GB instruments measuring at different LST or from satellites with drifting measurement schedules has shown a large variability. If the variation in ozone content vs LST is stable with years, the influence of the measurement schedule, as long as being constant, on the linear trend should be null and the variability of the trends could not be attributed to that effect. In the opposite case, we could explain part of the variability of the GB trends. With our study, we find a non significant variation of trend with LST, which is in line with the referee's guess, but allows to tell that a significant difference between the GB trends cannot be attributed to a constant measurement schedule difference.

Discrepancies between the post-1998 ozone profile trends calculated from ground-based instruments, satellite datasets and chemistry-climate models and the large uncertainties on the trends show that it is

difficult to clearly provide evidence of stratospheric ozone recovery (Steinbrecht et al., 2017; Ball et al., 2017; Petropavlovskikh et al., 2019). Besides information on the stability and drift of the measurements (Hubert et al., 2016), consideration of the ozone diurnal variability (Studer et al., 2014) and of the spatial and temporal sampling of the dataset (Damadeo et al., 2018) is of primary importance to understanding differences in the trends and to reduce the uncertainty associated with them. The variation of the trends with LST has to be quantified to calculate representative trends derived from sun-synchronous satellite measurements and ensure a proper comparison of these trends with those estimated from ground-based instruments, or to ensure a proper comparison of trends estimated from instruments with different measurement schedules. The consistent high time resolution of ground-based MWR instruments make them ideal for analysing this sampling bias.

Minor comments:
Please, see attached commented pdf.

p.1 line5:

5 Payerne MWR dataset has been homogenized ~~to ensure a stable measurement contribution~~ to the ozone ~~profiles and~~ to take

The precision is important here. We do not simply homogenize the timeseries by applying an offset on a part of the timeseries but we retrieve the ozone profiles after the technical intervention in order to get a similar measurement contribution before and after the intervention. We propose to keep the precision here.

p.1 line 12:

nighttime). The homogenized Payerne MWR [add short info what kind of dataset] within ±5% with the MLS dataset over the 30 to 65 km altitude range and within ±10% of HARMOZ datasets over the 30 to 65 km altitude range. In the upper stratosphere, there

As this is the abstract, we added here a very short information on the HARMOZ dataset.

…within +- 10% of the HARMonized dataset of OZone profiles (HARMOZ, limb and occultation measurements from Envisat).

Further, in section 2.3, we added:

The HARMOZ dataset (Sofieva et al, 2013) is based on limb and occultation measurements from Envisat (GOMOS, MIPAS and SCIAMACHY), Odin (OSIRIS, SMR) and SCISAT (ACE-FTS) satellite instruments providing ozone profiles in the altitude range from the upper troposphere up to the mesosphere in years 2001–2012.

p.1 line 15:

15 km is considered an instrumental artefact and is not further analyzed ~~and discussed.~~

We have changed this as suggested.

Hence, the induced bias at 55km is considered an instrumental artefact and is not further analyzed.

p.1 line 16:

In the upper stratosphere (5–1 hPa, 35–48 km), the Payerne MWR [add: but with a high variation with altitude] ~~trends are significantly positive~~ at 2 to 3 %/decade.

We have changed this as suggested.

The Payerne Switzerland microwave radiometer (MWR) ozone trends are significantly positive at 2 to 3 %/decade in the upper stratosphere (5–1hPa, 35–48km), with a high variation with altitude.

p.1 line 19:

what kind of variability you are speaking of? Between different datasets? Please specify

LOTUS project. The reason for variability in the reported long-term ground-based and satellite ozone profile trends has multiple

We have specified this as suggested.

In order to determine what part of the variability between different datasets comes from measurement timing, Payerne MWR and SOCOL v 3.0 chemistry-climate model (CCM) trends were estimated for each hour of the day with a multiple linear regression model.

p.2 line 25:

25 to a systematic temporal sampling. effect

Added as suggested.

Based on these results we conclude that significant trend differences between instruments cannot be attributed to a systematic temporal sampling effect.

p.2 line 27:

the

Since the discovery of the ozone hole over Antarctica in 1985 (Chubachi, 1985; Farman et al., 1985), understanding the

Added as suggested.

Since the discovery of the ozone hole over Antarctica in 1985 (Chubachi,1985, Farman et al.,1985), the understanding of the mechanisms that drive stratospheric ozone trends has been a major area of interest in atmospheric research.

p.2 line 34:

Chemical processes involved in polar ozone depletion also affect ozone in the stratosphere at a global scale (Solomon, 1999).

Besides the Chapman cycle

The main chemical species involved in stratospheric ozone loss processes are chlorine compounds (HCl, ClOx), hydroxyl

Added as suggested.

Besides the Chapman cycle, the main chemical species….

p.2 line 37:

1985; Solomon, 1999) since its first mention by Molina and S. (1974). In the stratosphere, the variability of NO_x plays a key

Please specify what kind of variability you mean (in time, in space, what scales)

role in the variability of ozone (Hendrick et al., 2012; Nedoluha et al., 2015a; Wang et al., 2014; E. et al., 2019). The NO_x

We have specified the kind of variability and added a value for the simulated conversion rate.

In the stratosphere, the variability in time of the amount of NOx plays a key role in the variability of ozone (Hendrick et al., 2012; Nedoluha et al., 2015a; Wang et al., 2014;Galytska et al., 2019), with an ozone conversion rate of the Chapman cycle of -0.25 ppmv/h (Schanz et al., 2014).

p.2 line 38:

1985; Solomon, 1999) since its first mention by Molina and S. (1974). In the stratosphere, the variability of NO_x plays a key role in the variability of ozone (Hendrick et al., 2012; Nedoluha et al., 2015a; Wang et al., 2014; E. et al., 2019). The NO_x

Please specify what kind of variability you mean (in time, in space, what scales)

The typo in the reference has been corrected.

…variability of ozone (Hendrick et al., 2012; Nedoluha et al., 2015a; Wang et al., 2014;Galytska et al., 2019).

p.3 line 58:

magnitude are datasets dependent. The persistent negative trends are likely a consequence of radiative and dynamical forcing from climate change (Chipperfield et al., 2017). In the tropical upper stratosphere trends are also positive, even if smaller than those in the mid-latitudes.

what is first? what exactly do you mean? I would say, that in contrast to the other parts of the stratosphere, here the change of the circulation, i.e. the acceleration of the BDC is the main driver (a kind of tele-impact) whereas otherwise local conditions (T, concentrations of trace gases) are the determining factors

By “dynamical forcing”, we exactly mean the change in the circulation driven by climate change. With “radiative”, we mean that the cooling of the stratosphere has an impact on the Brewer-Dobson circulation. We modified the sentence for clarity and kept only the “dynamical forcing”.

The persistent negative trends are likely a consequence of dynamical forcing from climate change (Chipperfield et al, 2017).

p.3 line 74:

trends estimated from instruments with different measurement schedules. The consistent high time resolution of ground-based MWR instruments make them ideal for excluding this sampling bias from the parameters influencing trend estimates.

analysing

We have changed this as suggested.

The consistent high time resolution of ground-based MWR instruments make them ideal for analysing this sampling bias.

p.3 line 77:

post-2000 linear trend by calculating long-term trends for each hour of the day and night with a multiple linear regression

after the year 2000

We have changed this as suggested.

…on the linear trend after the year 2000 by calculating…

p.4 line 113:

(1990)). Radiosonde and MLS data are blended in the tropospheric transition region. The ML climatology is combined with the Keating standard profile in the mesospheric transition region.

reference

A reference has been added as suggested.

The ML climatology is combined with the Keating standard profile (Keating et al., 1990) in the mesospheric transition region.

p.4 line 122:

contribution is higher than 80%. Figure 1 shows the Payerne MWR AVKs and the MC ($\times 0.5$) for one sample month (January 2013).

As a non-specialist for MWR observations, I wonder how the MC can be greater than 100% (Fig. 1 @20km). Please define MC more exactly. What about uncertainties? Are the shown AVKs and MC a mean profile?

The measurement contribution at a specific altitude is defined as the area of the averaging kernel corresponding to this specific altitude. Higher than 100% measurement response values are due to bigger than 1 area of the averaging kernel for that altitude. The ozone content at an altitude is not only sensitive to variations at that altitude, but also to concentrations at other altitudes because of the vertical resolution of the retrieved profile being coarser than the retrieval grid. This is often seen for ground-based instruments (MWR in Ryan et al., 2016 and Moreira et al., 2015) and to some extent for satellites (MLS in Livesey et al., 2018).

Ryan, N. J., Walker, K. A., Raffalski, U., Kivi, R., Gross, J., and Manney, G. L.: Ozone profiles above Kiruna from two ground-based radiometers, Atmos. Meas. Tech., 9, 4503–4519, https://doi.org/10.5194/amt-9-4503-2016, 2016.

The measurement contribution and AVK shown in Figure 1 are mean values for January 2013. A shaded area standing for the standard error of the mean has been added to the measurement contribution plot in Figure 1. The caption has been modified to mention that the plotted AVK and measurement contribution are means for January 2013.

Figure 1 shows the Payerne MWR AVKs mean and the MC mean (×0.5) for one sample month (January 2013).

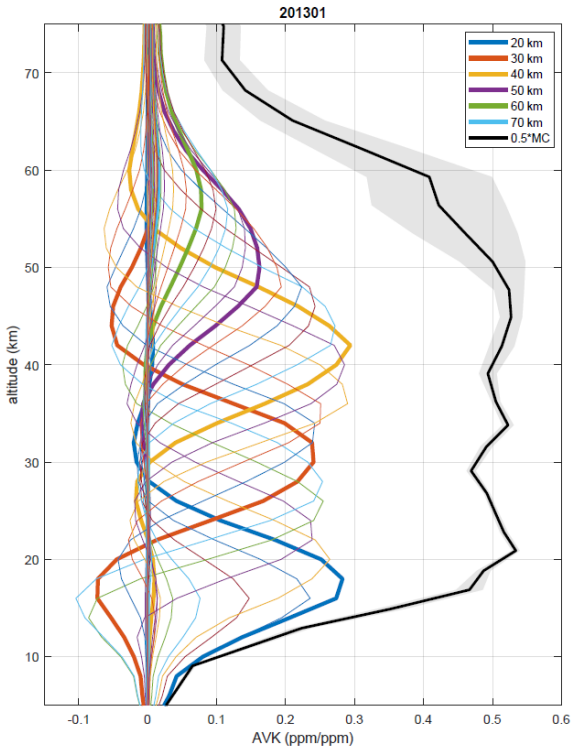

Figure 1. Mean values of Payerne MWR averaging kernels in ppm/ppm and measurement contribution (×0.5) for January, 2013. The shaded area represents the standard errors of the mean.

p.5 line 143:

pared for the overlap period of one year. In Fig. 2 the monthly means of the measurement contribution at 0.4 hPa as a % of the ozone profile are plotted against the monthly means of the diurnal cycle amplitude (maximum-to-minimum difference) as a % of the midnight ozone value for the 2000-2016 measurement period. A clear negative correlation between the amplitude of the

I would have expected you show differences for that year. Please motivate what you are doing.

We compare the measurement contributions of simultaneous ozone profiles retrieved from the AOS and FFTS measurements for the overlap period of one year and they are different when considering the same integration time. Instead of showing this difference here, we want to highlight the influence of such a difference on the ozone content with the particular case of the diurnal cycle, which is an essential ozone variation vs LST in the low mesosphere. The stability in time of the diurnal cycle measurement conditions is crucial for our long-term trend vs LST study.

The measurement contributions to simultaneous ozone profiles retrieved from the AOS and FFTS measurements were compared for the overlap period of one year and found to be different when considering the same integration time (not shown). In order to assess the influence of such a difference on the ozone content, the monthly means of the measurement contribution at 0.4 hPa as a % of the ozone profile are plotted in Fig. 2 against the monthly means of the diurnal cycle amplitude (maximum-to-minimum difference) as a % of the midnight ozone value for the 2000-2016 measurement period.

p. 6 line 150:

tion of the characteristics of the retrieval (measurement response and vertical resolution). The AOS and FFTS ozone profile
150 datasets used in this study were harmonized by ensuring a constant measurement contribution to the retrieved ozone profiles between 47 and 0.05 hPa (20 and 70km). The integration time for one ozone profile therefore varies from 30 min to 2 h.

what do you mean with constant? In time? or between altitude range?

We mean that for each single layer of the ozone profile, the MC value does not vary in time. Precision has been given on the measurement contribution evolution.

The AOS and FFTS ozone profile datasets used in this study were harmonized by ensuring a constant measurement contribution in time to each layer of the retrieved ozone profiles between 47 and 0.05 hPa (20 and 70 km).

p.6 line 156-8:

where high time resolution without any degradation of the measurement contribution is required. The FFTS2h data are used for the lower mesosphere where the consistency of the measurement contribution is more important than the time resolution requirement.

what about the AOS?

The measurement contribution of the AOS dataset is the reference and the time integration for the FFT dataset profiles has been adapted in order to get a consistency of the measurement contribution through the transition. We do not question the measurement contribution of the AOS dataset, only the stability of the measurement contribution through the AOS-FFT transition.

p.6 line 170:

correction offset is lower during daytime than during nighttime, following the diurnal variation of ozone. A correction offset depending on the LST has to be applied to the AOS data above 50 km for a proper homogenization of time series when LST depending monthly means are considered. Can you explain that behaviour?

Yes, we can explain the behavior as follow: Each of the technical upgrade influences the measurement contribution function of the ozone profile in a non-linear way. The resulting offset will depend on the altitude and on the amount of ozone. As, above 50 km, the ozone intensity varies with LST (up to 25%), the offset will follow a similar behavior. We added this explanation in the manuscript.

…when LST depending monthly means are considered. The AOS to FFTS spectrometer upgrade influences the measurement contribution function of the ozone profile in a non-linear way. The resulting offset will depend on the altitude and on the amount of ozone. As, above 50 km, the ozone intensity varies with LST (diurnal cycle up to 25%), the offset is presenting a similar behavior.

p.7 line 189:

in (Hubert et al., 2016; Hubert, 2019) a

The typo has been corrected.

Note that the mean drifts of 5-10 %/decade measured between the MWRs and the satellites shown in Hubert et al. (2016) and Hubert (2019) are not representative of the drifts during the two year periods considered here.

p.7 line 200:

means for altitudes below 50km, and the FFTS 2010-2018 timeseries of 2h LST-resolved monthly means for altitudes above 50km. In order to show the effect of homogenization, please show the deseasonalized timeseries before and after.

A figure (Fig. 4 of the updated manuscript version) showing the deseasonalized timeseries has been added. See General remark section of the review.

p.11 line 314:

$r(t)$ is the residual ~~noise~~, c_0 the linear component (the trend), and a the ordinate intercept of the regression line. The data

We have changed this as suggested.

…*r(t)* is the residual, c_0 the…

p.13 line 393:

Up to 50 km the 2000-2018 24-hour trend estimates are similar at the 95% confidence level to the 2000-2016 trend profiles of daily mean

We prefer the term “24-hour trend” to “daily mean trend” to avoid confusion with the “daytime trend” term.

p.13 line 394-6:

et al. (2019) (In Fig. 6, caption is not sufficient (1sig lines?, shaded aera full range or what?) Legends font size too small ly positive. For this study, we extended the time range by 2 years. Effects on trends can be noticed below 50 km with a shift towards more p ic trends do not vary significantly. At 50 km, the 24-hour average Payerne MWR trend is 2% dec lower than the trends calculated

Please re-arrange: At 2 hPa the trend is with 2%/dec significantly positive.

We tested the effect of the extended time span on the results:

The change of sign in the trend is a hint to understimated errors in trend estimating? Or a special year?

Style: 2%/dec or 2%/10y (see Fig).

Caption of Fig. 6 (Fig 7 in the updated version) has been modified.

We are very grateful to the referee for having pointed out a problem in the 2000-2016 trend values below 30 km: this is an error. There was obviously an inconsistency between 2000-2016 trends in Figure 6 and 2000-2016 daytime and nighttime trends in Figure 7 (c) and (d), which has been resolved by double checking the 2000-2016 trends plotted in Figure 6. The values plotted in Figure 6 comes from a different version of the dataset, and did not correspond to the trend described in the paper as a "shift towards more positive values". The 2000-2016 trends values in Fig.6 (now Fig.7) and Fig.7 (c) and (d) (now Fig.8 (c) and (d)) are now coherent, the slight difference between the 2 figures being attributed to the data outside the 10-14h and 22-2h time range, which are included in Figure 6 trend profiles but not in a mean of Figure 7 (c) and (d) trend profiles. We changed Figure 6, but did not make any modification to the text "shift towards more positive values", which is now describing the correct trend profiles.

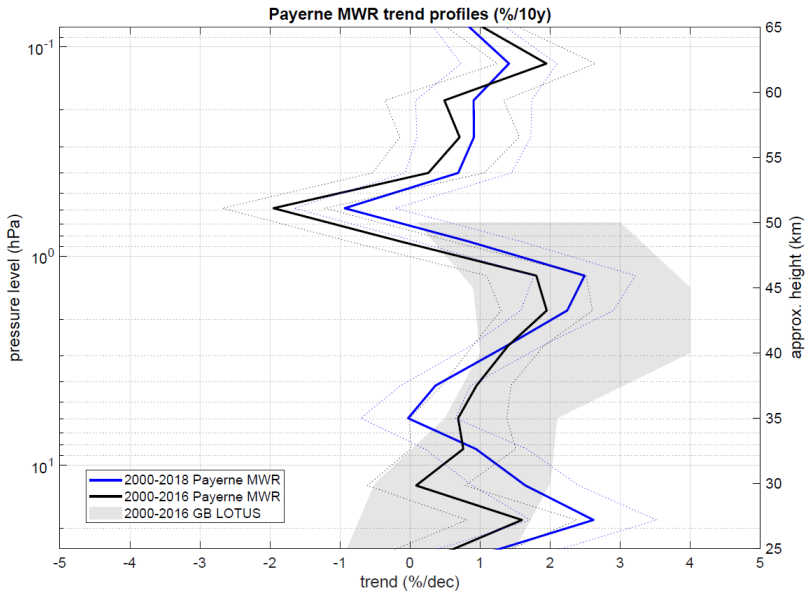

Figure 7. Payerne MWR O3 trend profiles for 2000-2016 time range in black and 2000-2018 time range in blue. The dotted lines show the 2σ uncertainties. The shaded area is the full range of LOTUS Ground-based 2000-2016 trend profiles.

The sentences have been modified and re-arranged as suggested. The term "/dec" has been replaced by "/10y" everywhere.

At 2 hPa (43 km) trend is with 2%/10y significantly positive. We tested the effect of the extended time span on the results. Effects on trends can be noticed below 30 km with a shift towards more positive values, while upper stratospheric trends do not vary significantly.

p. 14 line: 427:

In the stratosphere the ozone diurnal cycle shows presents a minimum at sunrise (~12.5 hPa) and a maximum (~4.16 hPa) in the

We have changed this as suggested.

…the ozone diurnal cycle shows a minimum…

p. 15 line 441:

Based on the correlation between ~~the~~ stratospheric O3 and ~~the~~ NOx, the active H and

We have changed this as suggested.

Based on the correlation between stratospheric O3 and NOx, the active ….

p.15 line 447:

Figure 9a shows the linear trends as a function of LST. [of ???]

We have completed the sentence.

Figure 10a shows the SOCOL OH linear trends as a function of LST.

p.15 line 453:

mainly influenced by temperature, thus the nighttime ozone trend simulated by SOCOL should be related to the temperature trends (Fig. 9c) [b)] and not to the OH trends.

The typo has been corrected.

…temperature trends (Fig. 10b) and not…

p.16 line 480:

480 Adding two more years to the dataset was shown to increase the trends below 30 km. A MLR was also applied to the high [this statement is a little bit misleading: trend changes its sign!]

See answer to referee's remark "p.13 line 394-6".

Answers to Referee nr 2:

The manuscript "Study of the dependence of stratospheric ozone long-term trends on local solar time" by Maillard Barras et al. describes homogenized long-term ozone time series from the SOMORA microwave radiometer in Payerne, Switzerland, including comparisons with other ground-based and satellite ozone datasets, and also simulations with the SOCOL v3.0 chemistry-climate model. Additionally, a trend analysis on all datasets is performed, with respect to local solar time, which becomes very important in the upper stratosphere and mesosphere. This analysis aims to answer the question if measurement timing could be the cause for trend variability within different observational datasets in the mesosphere, and therefore also aims to reduce the uncertainty on a possible ozone recovery signal in the regions of the atmosphere where the diurnal cycle in ozone is significant. The manuscript is very well written, and well structured. Its analysis is relevant to the community and fully within the scope of ACP. There are only a few minor things I would recommend the authors to consider before the manuscript can be published.

Thank you very much for your positive feedback. We consider your remarks and questions in the following.

General remarks:

• It might be helpful to describe the actual calculation of the bias a little more in detail. On page 2, lines 159-161 for example, it does not become totally clear if the bias correction was applied to each individual profile or an aggregated profile (e.g. monthly mean). And it is not clear if the bias actually is a value for each specific pressure level, or if it is time dependent.

We modified the description of the homogenization in order to clarify these points: The bias correction for the AOS-FFT transition (p 6 lines 159-161) was calculated and applied to aggregated profiles (monthly

means), and the bias correction value has been determined for each pressure level and respectively applied to each pressure level. In addition to the pressure level dependence, the time dependence (LST dependence) of the correction factor has been calculated for the AOS-FFT transition, the Front-End and GUNN technical upgrades using monthly means of simultaneous Payerne and Bern MWRs measurements. As the correction factor do not vary with LST in the stratosphere, no LST dependent correction factor has been applied to the timeseries in the stratosphere. In the low mesosphere, we show that a LST dependent correction factor should be applied for a proper homogenization of the timeseries.

The bias between the profiles retrieved from the two spectral measurement setups was then determined from monthly means of simultaneous measurements during the one year transition period. The mean absolute difference for each profile layer was subtracted from the aggregated AOS profiles, keeping the FFTS profile dataset unchanged. The bias correction values have been determined for each pressure level and respectively applied to each pressure level. Bias values are within 10% between 47 and 0.05 hPa (20 to 70km).
The application range of the correction offset depends to a large extent on the way the offset is calculated. The AOS to FFTS correction offset, when determined by the comparison of simultaneous monthly means, should be applied only to the global monthly means time series and not to sub-daily monthly means. In addition to the pressure level dependence, the time dependence (LST dependence) of the correction factor has been determined for the AOS to FFTS transition (for both the 1h and 2h bins) using monthly means of simultaneous Payerne and Bern MWRs measurements. As shown in Fig. 3a and b, the correction offsets do not vary significantly with LST below 50 km (0.6 hPa). No LST dependent correction factor has then been applied to the monthly means timeseries in the stratosphere. However, in the lower mesosphere, the AOS to FFTS 2h correction offset is lower during daytime than during nighttime, following the diurnal variation of ozone. A correction offset depending on the LST has to be applied to the AOS data above 50 km for a proper homogenization of time series when LST depending monthly means are considered.

• *Section 2: the mixture between the description of the different data sets, and the homogenization work performed on the Payerne data set was slightly confusing. I think it might be better to separate the two, in a data set description only section (where all the other datasets are described as well), and a separate homogenization section.*

A section has been added describing the homogenization of the Payerne MWR (Section 3). The homogenization description has been separated from the datasets description.

3 Homogenization of the Payerne MWR dataset

The homogenization of the Payerne MWR dataset was performed in stages. First, the integration time has been adapted at each … in the low mesosphere (0.27 hPa, 57 km).

• *Is there a reason why the conversion from ozone number density to ppm was done with ECMWF temperature profiles rather than the temperature profiles provided with HARMOZ? It might be worth adding a sentence or two for the reasoning of this to the manuscript.*

In (Hubert, 2016), the role of the auxiliary pressure and temperature profiles used for the unit conversion and for the vertical coordinate change is pointed out when investigating the differences between satellites ozone profiles. Therefore, we used a common T profiles dataset for the unit conversion and the vertical coordinate change before the convolution of the satellite datasets by the Payerne MWR. A sentence has been added in the manuscript to describe this step.

… conversion from number density (HARMOZ dataset) to ppm is carried out using ECMWF temperature profiles as a common auxiliary temperature profiles. The auxiliary pressure and temperature profiles used

for the unit conversion and for the vertical coordinate change influence the satellites ozone profiles difference as pointed out in Hubert et al. (2016).

• Page 13, line 387: I think the description of "the good agreement between the Payerne MWR and SOCOL v3.0" is very optimistic when looking at Figure 4. The differences between Payerne MWR and SOCOL range from -12% to +15% in the altitude range from 30-50km with a strong gradient. I think it would be more realistic to describe the agreement a little less optimistic.

The agreement between the Payerne MWR and SOCOL v3.0 has been described in a more realistic way.

Despite a modest agreement between the Payerne MWR and SOCOL v3.0 ozone content values, especially above 50 km, the good agreement between the Payerne MWR and SOCOL v3.0 diurnal variations in the 30 to 50 km altitude range make it possible to consider the comparison of both datasets variation with LST.

Specific remarks:
• Page 2, line 37: reference "Molina and S." seems to be abbreviated

The typo in the reference has been corrected.

… its first mention by Molina and Rowland (1974).

• Page 2, line 38: reference "E. et al." seems to be abbreviated

The typo in the reference has been corrected.

In the stratosphere, the variability of NO_x plays a key role in the variability of ozone (Hendrick et al., 2012; Nedoluha et al., 2015a; Wang et al., 2014;Galytska et al., 2019).

• Page 6, line 173: "was" missing between "front-end changed"?

"was" has been added.

The front-end was changed in 2005, and the GUNN oscillator was repaired in 2009.

• Page 6, line 173: "was" missing between "oscillator repaired"?

"was" has been added.

The front-end was changed in 2005, and the GUNN oscillator was repaired in 2009.

• Page 7, line 189: brackets not necessary around "(Hubert et al., 2016; Hubert, 2019)".

The typo in the reference has been corrected.

Note that the mean drifts of 5-10 %/decade measured between the MWRs and the satellites shown in Hubert et al. (2016) and Hubert (2019) are not representative of the drifts during the two year periods considered here.

• Page 7, line 192: not clear on what temporal resolution the offset application is based on.

The offset is calculated for each bin of 1 h (Fig 3 a,c,d) and of 2 h (Fig 3b)
Precision has been added in the manuscript (see answer to 1st remark in section "general remark" of referee 2).

Correction offsets have been evaluated by considering the 1h time bins.

• *Page 8, line 243: remove "to" in "from to 2.5"*

We have changed this as suggested.

MLS measures ozone profiles from 10 to 75 km with the vertical resolution ranging from 2.5 to 4 km.

• *Page 9, line 264: "converted" should be "conversion"?*

We have changed this as suggested.

… and conversion from number density (HARMOZ dataset) to ppm is carried out using ECMWF temperature profiles as a common auxiliary temperature profiles.

• *Page 10, line 279: the sentence part "chemical species interacting participating" seems weird and might need rewording.*

The word "interacting" has been removed.

Original version includes 41 chemical species participating in 140 gas-phase, …

• *Page 11, line 334: typo in the word "satellite"*

The typo has been corrected.

…comparing ground-based and satellite datasets…

• *Page 12, line 343: it might be helpful to actually give the latitude and longitude values of the box here to make it easier for the reader to understand the box' extension.*

The (min Longitude, min Latitude, max Longitude, max Latitude) coordinates values have been added.

Reducing the spatial coincidence criterion from 10◦ to 6◦ in latitude (reducing the box from (1.95°E,41.82°N,11.95°E,51.82°N) to (1.95°E,43.82°N,11.95°E,49.82°N)) reduces the number ….

• *Page 12, line 344: there might be a "that" missing in "means a"*

The word "that" has been added.

The high density of the MLS measurements means that a reduced area can be used…

• *Page 12, Section 4.1.1.1: It would be helpful to mention here again that the description of the differences is still a description of the results presented in Figure 4.*

This has been mentioned as suggested.

The mean relative difference between the Bern and Payerne MWRs lies between ±10% up to 40km, increasing up to a maximum of -10 to -13% between 47–57 km (Fig.5).

• *Page 13, line 375: remove "s" from "appears"*

We have changed this as suggested.

The relative differences also appear to vary with season, with ozone values being closer in NH winter than in summer (not shown).

• Page 13, line 375: the differences being smaller in" NH winter than in summer" is not shown in any figure, right? Would be worth mentioning that here (e.g. adding a "not shown") if you do not want to show these differences.

"Not shown" is now mentioned as suggested.

The relative differences also appear to vary with season, with ozone values being closer in NH winter than in summer (not shown).

• Page 13, line 389: "desagreement" should be "disagreement"

We have changed this as suggested.

Nevertheless, the disagreement in the height of the diurnal cycle extremes has to be considered when comparing trends.

• Page 14, line 427-430: If I understand correctly, you used the MLR described in Section 3.2 for the analysis described in Section 4.2.2. Is there a good reason to include ENSO and NOA basis functions in an ozone regression in the mesosphere?

ENSO and NOA do not have any significant contribution in the mesosphere (see plot below). ENSO and NAO however have a significant contribution in the middle stratosphere. For the sake of homogeneity in the trend retrieval, we decided to consider the same regressors for the whole altitude range and let the MLR procedure attribute the contributions to the regressors.

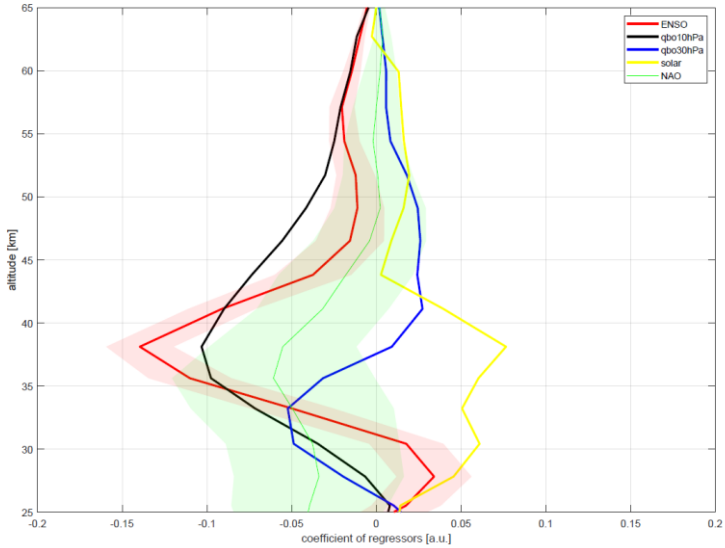

Figure: Profiles of ENSO, NAO, solar cycle and QBO regressors coefficients of the ozone MLR.

• Page 15, Section 4.2.3: It is not clear exactly what basis functions you used for NOx (and why they would be different for NOx and T for example). In line 445 you mention that ENSO is included as basis function, but in line 459 it is not mentioned anymore.

Sorry for the confusion. The first mention of the regressors is correct. We removed the redondant text.

The same MLR was applied to monthly means of SOCOL simulated reactive NOx (NOx =NO+NO2) for the period 2000-2016.

Answer to Editor remark (ACPD phase):

line 376ff: It is not clear to me, what the averaging of the solar cycle over ony year does, because the local times for sunrise and sunset do change significantly over the year. That means that for one single day I would expect even a much faster ozone change on the top level at sun rise because of the low photochemical lifetime. Would it not be better to have an average diurnal cycle over a shorter period? (This point may be left unchanged now and then could discussed in the normal ACPD discussion phase)

Averaging is necessary to reduce the noise and get a clear DC, however, you are right, the mesospheric DC is varying with the season as you can see in the figure below.

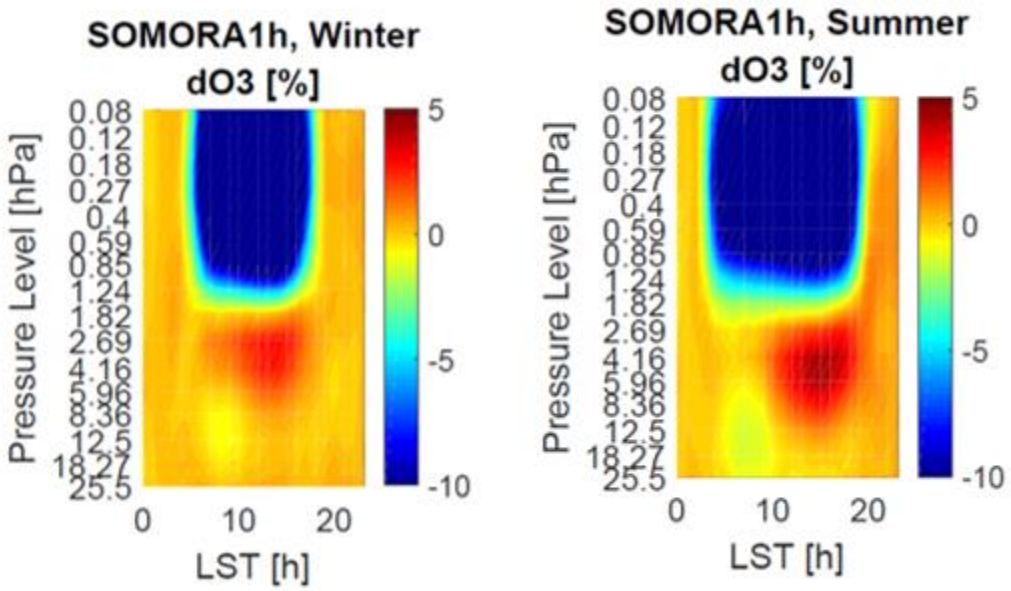

This has been published in Studer et al (https://doi.org/10.5194/acp-14-5905-2014). Here, we don't want to repeat a similar study, and we decided to show the similarities between the DC measured by MWR and simulated by SOCOL, similarities which are constant over the seasons.

Study of the dependence of stratospheric ozone long-term trends on local solar time

Eliane Maillard Barras[1], Alexander Haefele[1], Liliane Nguyen[2], Fiona Tummon[1], William T. Ball[3,4], Eugene V. Rozanov[4], Rolf Rüfenacht[1], Klemens Hocke[5], Leonie Bernet[5], Niklaus Kämpfer[5], Gerald Nedoluha[6], and Ian Boyd[7]

[1]Federal Office of Meteorology and Climatology, MeteoSwiss, Switzerland
[2]ISE, Institute for Environmental Sciences, University of Geneva, Switzerland
[3]Institute for Atmospheric and Climate Science, Swiss Federal Institute of Technology Zurich, Switzerland
[4]Physikalisch-Meteorologisches Observatorium Davos World Radiation Centre, Switzerland
[5]Institute of Applied Physics and Oeschger Centre for Climate Change Research, University of Bern, Bern, Switzerland
[6]Naval Research Laboratory, Washington DC, USA
[7]BC Scientific Consulting LLC, New Zealand

Correspondence: Eliane Maillard Barras (eliane.maillard@meteoswiss.ch)

Abstract.

Reliable ozone trends after 2000 are essential to ~~assess~~ detect early ozone recovery. However, the long-term ~~stability of data records by estimating the drift and bias of instruments. The ozone profile dataset from the SOMORA~~ ground-based and satellite ozone profile trends reported in the literature show a high variability. The reason for variability in the reported long-term trends has multiple possibilities such as the measurement timing and the dataset quality.

The Payerne Switzerland microwave radiometer (MWR) ~~in Payerne, Switzerland, was compared with profiles from the GROMOS MWR in Bern, Switzerland, satellite instruments (MLS, MIPAS, HALOE, SCHIAMACHY, GOMOS), and profiles simulated by the SOCOL v3.0~~ ozone trends are significantly positive at 2 to 3 %/decade in the upper stratosphere (5–1 hPa, 35–48 km), with a high variation with altitude. This is in accordance with the northern hemisphere (NH) trends reported by other ground-based instruments in the SPARC LOTUS project. In order to determine what part of the variability between different datasets comes from measurement timing, Payerne MWR and SOCOL v 3.0 chemistry-climate ~~model (CCM)~~model (CCM) trends were estimated for each hour of the day with a multiple linear regression model. Trends were quantified as a function of local solar time (LST). In the mid- and upper stratosphere, differences as a function of LST are reported for both the MWR and simulated trends for the post-2000 period. However, these differences are not significant at the 95% confidence level. In the lower mesosphere (1–0.1 hPa, 48–65 km), the 2010–2018 day- and nighttime trends have been considered. Here again, the variation of the trend with LST is not significant at the 95% confidence level. Based on these results we conclude that significant trend differences between instruments cannot be attributed to a systematic temporal sampling effect.

The dataset quality is of primary importance in a reliable trend derivation and multi-instrument comparison analyses can be used to assess the long-term stability of data records by estimating the drift and bias of instruments. The Payerne MWR dataset has been homogenized to ensure a stable measurement contribution to the ozone profiles and to take into account the effects of three major instrument upgrades. At each instrument upgrades, a correction offset has been calculated using parallel

measurements or simultaneous measurements by an independent instrument. At pressure levels smaller than 0.59 hPa (above ∼50 km), the homogenization corrections to be applied to the Payerne MWR ozone profiles are dependent on local solar time (LST). Due to the lack of reference measurements with a comparable measurement contribution at a high time resolution, a comprehensive homogenization of the sub-daily ozone profiles was possible only for pressure levels larger than 0.59 hPa.

The ozone profile dataset from the Payerne MWR, Switzerland, was compared with profiles from the GROMOS MWR in Bern, Switzerland, satellite instruments (MLS, MIPAS, HALOE, SCHIAMACHY, GOMOS), and profiles simulated by the SOCOL v3.0 CCM. The long-term stability and mean biases of the time series were estimated as a function of the measurement time (day- and nighttime). The homogenized Payerne MWR ozone dataset agrees within ±5% with the MLS dataset over the 30 to 65 km altitude range and within ±10% of ~~HARMOZ datasets~~ the HARMonized dataset of OZone profiles (HARMOZ, limb and occultation measurements from ENVISAT) over the 30 to 65 km altitude range. In the upper stratosphere, there is a large nighttime difference between Payerne MWR and other datasets, which is likely a result of the mesospheric signal aliasing with lower levels in the stratosphere due to a lower vertical resolution at that altitude. Hence, the induced bias at 55 km is considered an instrumental artefact and is not fur~~ther analyzed~~and discussed.

~~In the upper stratosphere (5–1 , 35–48), the Payerne MWR trends are significantly positive at 2 to 3 %/decade. This is in accordance with the northern hemisphere (NH) trends reported by other ground-based instruments in the SPARC LOTUS project. The reason for variability in the reported long-term ground-based and satellite ozone profile trends has multiple possibilities. To determine what part of the variability comes from measurement timing, MWR trends were estimated for each hour of the day with a multiple linear regression model to quantify trends as a function of LST. In the mid- and upper stratosphere, differences as a function of LST are reported for both the MWR and simulated trends for the 2000-2016 period. However, these differences are not significant at the 95% confidence level. In the lower mesosphere (1–0.1 , 48–65), the 2010-2018 day- and nighttime trends have been considered. Here again, the variation of the trend with LST is not significant at the 95% confidence level. Based on these results we conclude that trend differences between instruments cannot to be attributed to a systematic temporal sampling.~~

1 Introduction

Since the discovery of the ozone hole over Antarctica in 1985 (Chubachi, 1985; Farman et al., 1985), ~~understanding~~ the understanding of the mechanisms that drive stratospheric ozone trends has been a major area of interest in atmospheric research. After the first insights into the impacts of the Montreal Protocol on stratospheric ozone variability (Mäder et al., 2010, and references therein), the challenge is now to confirm the efficacy of the Montreal protocol by assessing stratospheric ozone recovery. Moreover, as ozone recovery is strongly influenced by climate change (Eyring et al., 2010; Meul et al., 2016), the continued monitoring of stratospheric ozone and its vertical structure is essential.

Chemical processes involved in polar ozone depletion also affect ozone in the stratosphere at a global scale (Solomon, 1999). ~~The~~ Beside the Chapman cycle, the main chemical species involved in stratospheric ozone loss processes are chlorine compounds (HCl, ClOx), hydroxyl radicals (OH), and nitrogen oxides (NO_x), while stratospheric temperature (T) influences

the rate of both ozone production and destruction. The effect of chlorine compounds on ozone loss has been extensively described in the literature (Farman et al., 1985; Solomon, 1999) since its first mention by Molina and Rowland (1974). In the stratosphere, the variability of NO_x plays a key role in the variability of ozone (Hendrick et al., 2012; Nedoluha et al., 2015a; Wang et al., 2014; Galytska et al., 2019), with an ozone conversion rate of the Chapman cycle of -0.25 $\mathrm{ppmv/h}$ (Schanz et al., 2014). The NO_x catalytic cycle counteracts the accumulation of ozone during the day and leads to a negative correlation between anomalies in NO_x and the amplitude of the ozone diurnal cycle (Schanz et al., 2014). Finally, the negative correlation of ozone and temperature is mainly due to the temperature dependence of the rate coefficients of the Chapman cycle reactions (Barnett et al., 1975; Craig and Ohring, 1958).

In the mesosphere, OH radicals destroy ozone in auto-catalytic cycles and dominate the ozone budget above about 1 hPa (Lossow et al., 2019). Mesospheric OH is predominantly produced by the photo-dissociation of water vapor and OH_x measurements can be used as a proxy for mesospheric H_2O (Newnham et al., 2019). The interaction of ozone with mesospheric water vapor is further described in Flury et al. (2009), Haefele et al. (2008), and references therein.

In the northern hemisphere (NH), upper stratospheric ozone is reported to be increasing by 2–3 % per decade, due to both declining levels of ozone depleting substances and stratospheric cooling. These estimates are based on measurements from satellites and ground-based instruments as well as chemistry-climate models simulations (Petropavlovskikh et al., 2019). This recovery is statistically significant down to 4 hPa ($\sim$38 km), however, at altitudes below this level, NH mid-latitude trends are not statistically significant. For the lowermost stratosphere, they even vary considerably between datasets (Bernet et al., 2019) although there is evidence for ongoing negative trends in some NH regions (Ball et al., 2018, 2019). For the mesosphere, negative trends have been reported in Moreira et al. (2015) and Kyrölä et al. (2013). In the southern hemisphere (SH) mid-latitudes, satellites and ground-based datasets show statistically insignificant negative trends in the middle and lower stratosphere while upper stratospheric trends are significantly positive at 2% per decade mainly close to 2 hPa (Petropavlovskikh et al., 2019). In the tropics, a continuous decline in the middle and lower stratosphere is simulated by chemistry-climate models and negative trends are retrieved from ~~satellite-~~ satellite and ground-based measurements (Petropavlovskikh et al., 2019) which significance and magnitude are datasets dependent. The persistent negative trends are likely a consequence of ~~radiative and~~ dynamical forcing from climate change (Chipperfield et al., 2017). In the tropical upper stratosphere trends are also positive, even if smaller than those in the mid-latitudes.

Few studies report lower mesospheric (altitudes above 0.6 hPa) ozone trends based on measurements for the period after 1998. Moreira et al. (2015) report negative trends up to -4% per decade for the 1997–2015 period between 52 and 67 km in the NH. In Marsh et al. (2003), negative mesospheric long-term trends of -4% per year are derived from HALOE sunset (SS) measurements before 2003.

Discrepancies between the post-1998 ozone profile trends calculated from ground-based instruments, satellite datasets and chemistry-climate models and the large uncertainties on the trends show that it is difficult to clearly provide evidence of stratospheric ozone recovery (Steinbrecht et al., 2017; Ball et al., 2017; Petropavlovskikh et al., 2019). Besides information on the stability and drift of the measurements (Hubert et al., 2016), consideration of the ozone diurnal variability (Studer et al., 2014) and of the spatial and temporal sampling of the dataset (Damadeo et al., 2018) is of primary importance to

understanding differences in the trends and to reduce the uncertainty associated with them. The variation of the trends with LST has to be quantified to calculate representative trends derived from sun-synchronous satellite measurements and ensure a proper comparison of these trends with those estimated from ground-based instruments, or to ensure a proper comparison of trends estimated from instruments with different measurement schedules. The consistent high time resolution of ground-based MWR instruments make them ideal for ~~excluding~~ analysing this sampling bias~~from the parameters influencing trend estimates~~.

In this study, we first carefully homogenize the SOMORA Payerne MWR ozone profile dataset and validate this dataset against simultaneous ozone profiles measured by satellites. We then investigate the effect of the ozone diurnal cycle on the ~~post-2000 linear trend~~ linear trend after the year 2000 by calculating long-term trends for each hour of the day and night with a multiple linear regression (MLR) model. Finally we compare the SOMORA Payerne MWR ozone trends in the upper and middle stratosphere to trends of OH, NO_x and T derived from the SOCOL v3.0 CCM, to investigate the correlations between the long-term variability of ozone, water vapor, nitrous oxide, and temperature, particularly at the diurnal scale.

The paper is organized as follows: Section 2 describes the ozone datasets measured by individual instruments. ~~Section 3~~ The homogenization of the Payerne MWR dataset is described in Section 3. Section 4 is dedicated to the description of the methods used to calculate the diurnal cycle and trends. In ~~Sect. 4~~Section 5, we describe and discuss the results of the SOMORA Payerne MWR validation and of the dependence of the MLR trends as a function of the time of day. Conclusions about the variability of the long-term stratospheric ozone trends are provided in ~~Sect. 5.~~ Section 6.

2 Data Sources

2.1 Stratospheric Ozone MOnitoring RAdiometer (SOMORA)

The microwave radiometer SOMORA, hereafter referred to as the Payerne MWR, is located in Payerne (46.82° N, 6.95° E, 491 m), Switzerland, and has been operated continuously by MeteoSwiss since January 2000. Ozone profile retrievals are obtained independent of weather conditions throughout the diurnal cycle, forming a dataset with a constant and stable time sampling over two decades. Ozone profiles are provided in volume mixing ratio (ppmv) on a pressure grid between 47.3 and 0.05 hPa. The vertical resolution is 8–10 km from 47 to 1.8 hPa (20 to 40 km), increasing to 15–20 km at 0.18 hPa (60 km) (Maillard Barras et al., 2015). The measurement contribution is above 80% from 47 to 0.27 hPa (20 to 57 km). The Payerne MWR is included in the Network for the Detection of Atmospheric Composition Change (NDACC).

2.1.1 Measurement principles and profile retrieval

Developed in 2000 by the University of Bern (Calisesi, 2000), the Payerne MWR is a total power microwave radiometer measuring the thermal emission line of ozone at 142.175 GHz. The electromagnetic radiation is measured at an antenna elevation angle of 39° and the brightness temperatures range from 80 to 260 K. The Payerne MWR is calibrated using a hot load heated and stabilized at 300 K and a cold load at 77 K cooled with liquid nitrogen. A rotating planar mirror is used as a switch between the radiation sources. A Martin-Puplett interferometer (sideband filter) picks out the frequency band

around 142 GHz. Outgoing from the front-end part (quasi optics), the signal is amplified and down-converted in frequency to 7.1 GHz (mixer) by means of a constant-frequency signal (GUNN oscillator). The signal is further down-converted in two steps (intermediate step at 1.5GHz/1GHz) to the baseband (0–1 GHz). The spectral distribution, i.e. voltage as a function of channel or frequency, is measured by Acousto-optical spectrometers (AOS) in the first decade and since then by an Acquiris Fast-Fourier-Transform spectrometer (FFTS) with 16384 channels distributed over 1GHz bandwidth.

The pressure broadening effect on the line allows the retrieval of the vertical ozone profile from the measured spectrum using an a priori profile, a radiative transfer simulation (forward model, ARTS (Buehler et al., 2005)), and the optimal estimation method (OEM, Qpack (Eriksson et al., 2005)) based on Rodgers (2000).

The required a priori information is taken from a monthly-varying climatology (called the ML climatology and described in McPeters and Labow (2012) formed by combining data from Aura MLS (2004-2010) with data from balloon radiosondes (1988-2010)). Ozone below 8 km is based on sonde measurements, from 16 km to 65 km it is based on MLS measurements, and above 65 km a climatological standard profile combining 5 satellite ozone datasets is used (described in Keating et al. (1990)). Radiosonde and MLS data are blended in the tropospheric transition region. The ML climatology is combined with the Keating standard profile (Keating et al., 1990) in the mesospheric transition region.

The diagonal elements of the a priori covariance matrix are given by the variance of the ML climatology. The off-diagonal elements are parameterized with an exponentially decaying correlation function using a correlation length of 3 km. The diagonal elements of the error covariance matrix of the measured spectrum are estimated from the variance of the wings of the measured spectrum. The off-diagonal elements of the measurement error covariance matrix are zero.

The retrieval is characterized by the averaging kernel (AVK) matrix describing the changes in the retrieved profile as a function of changes in the true profile. The width of the AVKs is a measure of the vertical resolution of the retrievals and the area of the AVKs indicates the measurement contribution to the retrieved profile (Rodgers, 2000). The ozone profile is considered as reliable when the measurement contribution (MC) dominates the a priori information, i.e. when the measurement contribution is higher than 80%. Figure 1 shows the Payerne MWR AVKs mean and the MC mean ($\times 0.5$) for one sample month (January 2013).

2.1.2 Data quality and reliability

The total uncertainty is calculated for each retrieved profile accounting for the following sources of uncertainty: measurement noise, tropospheric attenuation, calibration load temperatures, spectroscopy, atmospheric temperature profile, and smoothing. The dominant source of uncertainty is smoothing because of the instrument's limited vertical resolution and is on the order of 15-20% of the ozone content. The second most important contribution is the measurement noise on the spectra amounting to 3–7% error when using a standard integration time of 1 hour. Tropospheric attenuation correction, the pressure-broadening coefficient of the observed line, calibration loads temperatures, and the atmospheric temperature profile (Payerne radiosondes combined with the ECMWF ERA-interim data) amount to an uncertainty of less than 3%.

2.1.3 Homogenization

2.1.2.1 Homogenization of the Payerne MWR AOS and FFTS time series

Spectral analysis of the Payerne MWR measurements was performed using two acousto-optical spectrometers (AOS) from January 2000 to October 2010; the AOS had a total bandwidth of 1 GHz, with a frequency resolution varying from 24 kHz at the line center to 980 kHz at the wings. In September 2009, an Acquiris fast Fourier transform spectrometer (FFTS) was added as a back end to the Payerne MWR. The FFTS covers a total bandwidth of 1GHz with 16384 channels, providing a frequency resolution of 61 kHz. This technical upgrade introduced a discontinuity in the timeseries, requiring an homogenization of the dataset. The AOS and FFTS were used in parallel for one year to ensure a proper homogenization of the transition.

The measurement contributions to simultaneous ozone profiles retrieved from the AOS and FFTS measurements were compared for the overlap period of one year. In Fig. 2 the monthly means of the measurement contribution at 0.4 as a % of the ozone profile are plotted against the monthly means of the diurnal cycle amplitude (maximum-to-minimum difference) as a % of the midnight ozone value for the 2000-2016 measurement period. A clear negative correlation between the amplitude of the ozone diurnal cycle and the measurement contribution is shown for the lower mesosphere. A low measurement contribution means there is a large a priori contribution. Since the a priori profile is a standard climatological ozone profile without any diurnal variation, the lower the measurement contribution, the lower the diurnal cycle amplitude. Since the ozone diurnal cycle amplitude is correlated to the measurement contribution value, a proper homogenization should not be limited to a correction of the bias between profiles retrieved from the spectra measured by the 2 spectral setups but should include a full homogenization of the characteristics of the retrieval (measurement response and vertical resolution). The AOS and FFTS ozone profile datasets used in this study were harmonized by ensuring a constant measurement contribution to the retrieved ozone profiles between 47 and 0.05 (20 and 70). The integration time for one ozone profile therefore varies from 30 min to 2 h. For a stable measurement contribution over the AOS to FFTS transition in the upper stratosphere/lower mesosphere, FFTS measurements require being accumulated over 2 h (FFTS2h dataset). However, in the altitude range where the measurement contribution is much larger than 80%, a FFTS signal accumulation time of 1 h is sufficient, therefore allowing a higher time resolution dataset (FFTS1h dataset). The FFTS1h data are used for the middle stratosphere and upper stratosphere below 48where high time resolution without any degradation of the measurement contribution is required. The FFTS2h data are used for the lower mesosphere where the consistency of the measurement contribution is more important than the time resolution requirement.

The bias between the profiles retrieved from the two spectral measurement setups was then determined from simultaneous measurements during the one year transition period. The mean absolute difference for each profile layer was subtracted from the AOS profiles, keeping the FFTS profile dataset unchanged. Bias values are within 10% between 47 and 0.05 (20 to 70).

The application range of the correction offset depends to a large extent on the way the offset is calculated. The AOS to FFTS correction offset, when determined by the comparison of simultaneous monthly means, should be applied only to the global monthly means time series and not to sub-daily monthly means. To homogenise the AOS to FFTS datasets for both the 1h and 2h bins, the AOS to FFTS correction offset variation with LST was determined. As shown in Fig. 3a and b, the correction offsets do not vary significantly with LST below 50 (0.6). However, in the lower mesosphere, the AOS to FFTS 2h correction

offset is lower during daytime than during nighttime, following the diurnal variation of ozone. A correction offset depending on the LST has to be applied to the AOS data above 50 for a proper homogenization of time series when LST depending monthly means are considered.

2.1.2.1 Time series corrections for technical issues

Since January 2000 the Payerne MWR has been affected by several technical issues: the mixer diode was replaced in 2001, the front-end changed in 2005, and the GUNN oscillator repaired in 2009. Each of these major technical interventions could potentially affect the measured spectrum by modifying the baseline shape and the receiver temperature. The retrieval was adapted between the 2001 and 2005 interventions by considering a sinusoidal function in the spectrum background removal. For the correction of the effects from the 2005 and 2009 interventions, homogenization of the ozone profile time series was performed using coincident AVK convolved ozone profiles from the Bern MWR and AURA/MLS. The absolute mean differences of the coincident datasets were considered. For the 2005 homogenization, the difference between the Payerne MWR AOS dataset and the Bern MWR after the upgrade (in 2007, since in 2006 the Bern MWR dataset presents a negative anomaly compared to other instruments (Bernet et al., 2019)) was subtracted from the difference between the Payerne MWR AOS dataset and the Bern MWR before the upgrade (in 2004). This relative bias was then removed from the Payerne MWR profile dataset prior to the 2005 intervention. For the 2009 homogenization, the difference between the Payerne MWR AOS dataset and MLS in 2010 was subtracted from the difference between the Payerne MWR AOS dataset and MLS in 2008. This relative bias was then removed from the Payerne MWR profile dataset prior to the 2009 intervention. These homogenizations are only possible if it is assumed the reference instruments (i.e. the Bern MWR and MLS) do not drift during the periods considered. The Bern MWR dataset does not present any anomalies compared to other ground-based instruments in 2004 and 2007 (Bernet et al., 2019) and the MLS dataset does not present any anomalies compared to other satellite instruments between 2008 and 2010 (Hubert et al., 2016). Note that the mean drifts of 5-10%/decade measured between the MWRs and the satellites shown in (Hubert et al., 2016; Hubert, 2019) are not representative of the drifts during the two year periods considered here.

Here again, the 2005 and 2009 technical issues affect the ozone profiles above 50 differently depending on the LST. Figure 3c and d show the correction offset variation with LST for the 2005 and 2009 upgrades. Correction offsets have to be evaluated by considering the time bins. While a correction for 2005 is possible using the Bern MWR high time resolution dataset (Fig. 3c), in 2009 the lack of coincident measurements at high time resolution makes any LST-resolved correction very difficult (impossible). Coincident MLS measurements are available only twice a day (1 am and 1 pm overpasses) and the Bern MWR underwent an upgrade in 2009, meaning the stability of the dataset in term of measurement contribution during this particular period is uncertain (Fig. 3d).

A homogenised version of the 2000-2018 Payerne MWR dataset was thus made available for monthly means without any LST distinction above 50 . For this study, we used the homogenised 2000-2018 timeseries of 1h LST-resolved monthly means for altitudes below 50, and the FFTS 2010-2018 timeseries of 2h LST-resolved monthly means for altitudes above 50.

2.2 Other MWRs

2.2.1 GROMOS Bern microwave radiometer

The GROMOS (GROund-based Millimeter-wave Ozone Spectrometer) microwave radiometer, hereafter referred to as the Bern MWR, is a ground-based ozone microwave radiometer continuously observing the middle atmosphere above Bern (46.95° N, 7.44° E, 577 m), Switzerland, since November 1994. Like the Payerne MWR, the Bern MWR measures the thermal microwave emission of the rotational transition of ozone at 142.175 GHz, switching between the atmosphere, a cold load (liquid nitrogen at 80 K) and a hot load (electrical heater at 313 K). The Bern MWR spectral distribution has been measured since 1994 by a filter bank spectrometer with an integration time of 1h (frequency resolution of 100 MHz to 200 kHz) replaced in 2009 by an FFTS with an integration time of 30min (30.5 kHz frequency resolution). For technical details about the instrument, the measurement principle and the retrieval procedure, see Moreira et al. (2015) and Bernet et al. (2019, and references included therein). The vertical resolution is between 8–12 km in the stratosphere and increases with altitude to 20–25 km in the lower mesosphere. The measurement contribution is above 80% from 20 to 52 km Moreira et al. (2015). The Bern MWR also contributes to NDACC.

2.2.2 Mauna Loa MWR

The Mauna Loa MWR (MLO MWR) operated by U.S. the Naval Research Laboratory measures the emission spectrum of the ozone line at 110.836 GHz. It has been in operation at Mauna Loa (19.54° N, 155.6° W, 3397 m), USA, since 1995 and also contributes to NDACC. The spectral intensities are calibrated with black body sources at ambient and liquid nitrogen temperatures. The experimental technique is described in Parrish et al. (1992), and technical details about the instrument are provided in Parrish (1994). While the basic radiometric features are similar to the Bern and Payerne MWRs, the MLO MWR receiver is cryogenically cooled and the spectral distribution is measured by a filter bank spectrometer. The ozone mixing ratio profiles are retrieved from the spectra using an adaptation of the optimal estimation method of Rodgers (Connor et al., 1995; Rodgers, 2000).

The vertical resolution is 6 km at an altitude of 32 km, between 6 and 8 km from 20 to 42 km, and then increases to 14 km at 65 km. The measurement contribution is above 80% from 20 to 70 km. While hourly measurements are performed for the purpose of diurnal cycle studies (Parrish et al., 2014), data are deposited in the NDACC with a 6-hourly time resolution. The NDACC dataset is used in this study. The MLO MWR underwent a major spectrometer upgrade between 2015 and 2017. For this study, only data until May 2015 have been used.

2.3 Satellites

The Payerne MWR is compared to the three instruments from the ENVISAT satellite: GOMOS (Global Ozone Monitoring by Occultation of Stars), MIPAS (Michelson Interferometer for Passive Atmospheric Sounding) and SCIAMACHY (SCanning Imaging Absorption spectroMeter for Atmospheric CHartographY), as well as to the MLS (Microwave Limb Sounder) on the

Aura satellite and HALOE (Halogen Occultation Experiment) on the UARS satellite. The ENVISAT instruments are part of the Ozone Climate Change Initiative (Ozone CCI).

The HARMOZ dataset (Sofieva et al., 2013) is ~~composed of ENVISAT~~ based on limb and occultation measurements from ENVISAT (GOMOS, MIPAS and SCIAMACHY), Odin (OSIRIS, SMR) and SCISAT (ACE-FTS) satellite instruments providing ozone profiles in the altitude range from the upper troposphere up to the mesosphere in years 2001–2012. The ozone profiles are given in number density on a common pressure grid, which corresponds to a vertical sampling of 2–3 km.

HARMOZ and HALOE data centered 10° by 10° around Payerne were selected (equivalent to an area of approximately 1110 km by 760 km). The collocation criterion for MLS satellite data is ±3° in latitude and ±5° in longitude (an area of approximately 666 km by 760km). This criterion ensures a sufficient number of collocated measurements and thus provides reliable bias estimates.

2.3.1 MLS

MLS is a microwave limb-sounding radiometer onboard the Aura Earth observing satellite. Ozone profiles are retrieved from MLS radiance measurements at 240 GHz. Details about the Aura mission can be found in Waters et al. (2006). In this study we use ozone profiles from the version 4.2 dataset (Livesey, 2018). MLS measures ozone profiles from 10 to 75 km with the vertical resolution ranging from ~~to~~ 2.5 to 4 km. MLS passes over Payerne at 1:30 UTC and 13:30 UTC. For the comparison with coincident Payerne MWR ozone profiles, the MLS profiles are convolved to the Payerne MWR vertical resolution using AVKs.

2.3.2 ENVISAT

MIPAS is an infrared limb emission Fourier transform spectrometer (spectral range from 685 to 2410 cm^{-1}) on board the ENVISAT satellite. MIPAS provided profiles of H_2O, O_3, HNO_3, CH_4, N_2O and NO_2 from 2002 to 2012. Stratospheric ozone profiles are retrieved with the version V7R_O3_240 research processor developed at KIT IMK/IAA via constrained inverse modeling of limb radiances (Laeng et al., 2017). Data used in this study are the OR (Optimized Resolution) dataset from 2005 to 2012. MIPAS measured ozone profiles from 10–80 km, with a vertical resolution ranging from 2.4 km at an altitude of 10 km to 3.6 km at 30 km and 5 km at 70 km.

GOMOS was a stellar occultation instrument on board ENVISAT from 2002 to 2012 (Bertaux et al., 2010). GBL (Gomos Bright Light) measured the atmospheric limb radiance of scattered sunlight (Tukiainen et al., 2015). Ozone profiles are retrieved using the ESA IPF v6 processor (Sofieva et al., 2017) from the ultraviolet and visible spectrometer measurements at wavelengths between 250 and 692 nm with a two-step inversion (Kyrölä et al., 2010). ENVISAT overpass times for Payerne are 10:00 UTC (GBL dataset) and 22:00 UTC (GOMOS dataset). GOMOS measured ozone profiles from 20–100 km, with a vertical resolution of 2 km below altitudes of 30 km and 3 km above 40 km.

SCIAMACHY was a spaceborne spectrometer that measured the upwelling radiation from the Earth's atmosphere in the UV, visible, near-infrared and shortwave-infrared spectral ranges. A detailed description of the instrument and its measurement modes can be found in Bovensmann et al. (1999). Ozone profiles used in this study are retrieved using the UBR limb

retrieval algorithm (V3_5). SCIAMACHY measured ozone profiles from 15-40 km, with a vertical resolution of 3 km. While measuring, SCIAMACHY passed over Payerne at 10:00 UTC. The MIPAS, GOMOS, GBL and SCIAMACHY profiles are AVK-convolved to the vertical resolution of the Payerne MWR and ~~converted~~ conversion from number density (HARMOZ dataset) to ppm is carried out using ECMWF temperature profiles ~~.~~ as a common auxiliary temperature profiles. The auxiliary pressure and temperature profiles used for the unit conversion and for the vertical coordinate change influence the satellites ozone profiles difference as pointed out in Hubert et al. (2016).

2.3.3 HALOE

HALOE was a mid-infrared solar occultation instrument on board the UARS (Upper Atmosphere Research Satellite) from 1991 to 2005 (Russell et al., 1993). HALOE retrieved vertical profiles of O_3, HCl, HF, CH_4, H_2O, NO, NO_2, aerosols and temperature from 15 daily sunrise (SR) and sunset (SS) measurements equally spaced in longitude. Data used in this study are the third public release record (v19). HALOE measured ozone profiles from 15 to 80 km with a vertical resolution of 3–5 km. For comparison with coincident Payerne MWR ozone profiles, the HALOE profiles are AVK-convolved to the Payerne MWR vertical resolution.

2.4 SOCOL CCM

The SOlar Climate Ozone Links (SOCOL) CCM consists of the middle atmosphere version of the MA-ECHAM general circulation model (Roeckner et al., 2003; Giorgetta et al., 2006), with 39 vertical levels between the surface and 0.01 hPa (∼80 km) coupled to the Model for Evaluation of oZONe trends (MEZON) chemistry module (Egorova et al., 2003).Dynamical and physical processes in the CCM SOCOL are calculated every 15 minutes within the model, while full radiative and chemical calculations are performed every two hours. Chemical constituents are transported using a flux-form semi-Lagrangian scheme (Lin and Rood, 1996). Original version includes 41 chemical species ~~interacting~~ participating in 140 gas-phase, 46 photolysis, and 16 heterogeneous reactions. The CCM SOCOL exploits T42 horizontal spectral truncation, which corresponds approximately to 2.5° by 2.5° resolution. The first model version was described and evaluated by Stenke et al. (2013). The model now includes an isoprene oxidation mechanism (Poeschl et al., 2000), the online calculation of lightning NOx emissions (Price and Rind, 1992), treatment of the effects produced by different energetic particles (Rozanov et al., 2012), updated reaction rates and absorption cross sections (Sander, 2011), improved solar heating rates (Sukhodolov et al., 2014), as well as a parameterization of cloud effects on photolysis rates (Chang et al., 1987). All considered halogenated ozone depleting species are transported as separate tracers.

The SOCOL v3.0 dataset has been validated in the troposphere and stratosphere with satellites, NDACC ground-based instruments and other CCMs (Staehelin et al., 2017; Revell et al., 2015; Stenke et al., 2013). Stratospheric ozone trends derived from SOCOL v3.0 in specified dynamics mode have also been compared with trends derived from measurements (Ball et al., 2018). For the comparison with ground-based observations the model outputs were horizontally interpolated to the location of Payerne from the adjacent grid cells. An AVK convolution was also applied to the model data for comparison with the Payerne MWR profiles.

3 Homogenization of the Payerne MWR dataset

The homogenization of the Payerne MWR dataset was performed in stages. First, the integration time has been adapted at each upgrade transition to ensure a constant measurement contribution over the dataset time range. At the spectrometer upgrade transition (AOS to FFTS), a correction offset has been calculated over one year of simultaneous measurements. At the front-end and the Gunn oscillator upgrades transitions, the correction offsets have been calculated using simultaneous measurements by an independent instrument, resp. by the Bern MWR and by MLS satellite. Moreover, the homogenization corrections to be applied to the Payerne MWR ozone profiles are dependent on local solar time (LST).

3.1 Homogenization of the Payerne MWR AOS and FFTS time series

Spectral analysis of the Payerne MWR measurements was performed using two acousto-optical spectrometers (AOS) from January 2000 to October 2010; the AOS had a total bandwidth of 1 GHz, with a frequency resolution varying from 24 kHz at the line center to 980 kHz at the wings. In September 2009, an Acquiris fast Fourier transform spectrometer (FFTS) was added as a back end to the Payerne MWR. The FFTS covers a total bandwidth of 1GHz with 16384 channels, providing a frequency resolution of 61 kHz. This technical upgrade introduced a discontinuity in the timeseries, requiring an homogenization of the dataset. The AOS and FFTS were used in parallel for one year to ensure a proper homogenization of the transition.

The measurement contributions to simultaneous ozone profiles retrieved from the AOS and FFTS measurements were compared for the overlap period of one year and found to be different when considering the same integration time (not shown). In order to assess the influence of such a difference on the ozone content, the monthly means of the measurement contribution at 0.4 hPa as a % of the ozone profile are plotted in Fig. 2 against the monthly means of the diurnal cycle amplitude (maximum-to-minimum difference) as a % of the midnight ozone value for the 2000-2016 measurement period. A clear negative correlation between the amplitude of the ozone diurnal cycle and the measurement contribution is shown for the lower mesosphere. A low measurement contribution means there is a large a priori contribution. Since the a priori profile is a standard climatological ozone profile without any diurnal variation, the lower the measurement contribution, the lower the diurnal cycle amplitude. Since the ozone diurnal cycle amplitude is correlated to the measurement contribution value, a proper homogenization should not be limited to a correction of the bias between profiles retrieved from the spectra measured by the 2 spectral setups but should include a full homogenization of the characteristics of the retrieval (measurement response and vertical resolution). The AOS and FFTS ozone profile datasets used in this study were harmonized by ensuring a constant measurement contribution in time to each layer of the retrieved ozone profiles between 47 and 0.05 hPa (20 and 70 km). The integration time for one ozone profile therefore varies from 30 min to 2 h. For a stable measurement contribution over the AOS to FFTS transition in the upper stratosphere/lower mesosphere, FFTS measurements require being accumulated over 2 h (FFTS2h dataset). However, in the altitude range where the measurement contribution is much larger than 80%, a FFTS signal accumulation time of 1 h is sufficient, therefore allowing a higher time resolution dataset (FFTS1h dataset). The FFTS1h data are used for the middle stratosphere and upper stratosphere below 48 km where high time resolution without any degradation of the measurement contribution is

required. The FFTS2h data are used for the lower mesosphere where the consistency of the measurement contribution is more important than the time resolution requirement.

The bias between the profiles retrieved from the two spectral measurement setups was then determined from monthly means of simultaneous measurements during the one year transition period. The mean absolute difference for each profile layer was subtracted from the aggregated AOS profiles, keeping the FFTS profile dataset unchanged. The bias correction values have been determined for each pressure level and respectively applied to each pressure level. Bias values are within 10% between 47 and 0.05 hPa (20 to 70 km).

The application range of the correction offset depends to a large extent on the way the offset is calculated. The AOS to FFTS correction offset, when determined by the comparison of simultaneous monthly means, should be applied only to the global monthly means time series and not to sub-daily monthly means. In addition to the pressure level dependence, the time dependence (LST dependence) of the correction factor has been determined for the AOS to FFTS transition (for both the 1h and 2h bins) using monthly means of simultaneous Payerne and Bern MWRs measurements. As shown in Fig. 3a and b, the correction offsets do not vary significantly with LST below 50 km (0.6 hPa). No LST dependent correction factor has then been applied to the monthly means timeseries in the stratosphere. However, in the lower mesosphere, the AOS to FFTS 2h correction offset is lower during daytime than during nighttime, following the diurnal variation of ozone. A correction offset depending on the LST has to be applied to the AOS data above 50 km for a proper homogenization of time series when LST depending monthly means are considered. The AOS to FFTS spectrometer upgrade influences the measurement contribution function of the ozone profile in a non-linear way. The resulting offset will depend on the altitude and on the amount of ozone. As above 50 km, the ozone intensity varies with LST (diurnal cycle up to 25%), the offset is presenting a similar behavior.

3.2 Time series corrections for technical issues

Since January 2000 the Payerne MWR has been affected by several technical issues: the mixer diode was replaced in 2001, the front-end was changed in 2005, and the GUNN oscillator was repaired in 2009. Each of these major technical interventions could potentially affect the measured spectrum by modifying the baseline shape and the receiver temperature. The retrieval was adapted between the 2001 and 2005 interventions by considering a sinusoidal function in the spectrum background removal. For the correction of the effects from the 2005 and 2009 interventions, homogenization of the ozone profile time series was performed using coincident AVK convolved ozone profiles from the Bern MWR and AURA/MLS. The absolute mean differences of the coincident datasets were considered. For the 2005 homogenization, the difference between the Payerne MWR AOS dataset and the Bern MWR after the upgrade (in 2007, since in 2006 the Bern MWR dataset presents a negative anomaly compared to other instruments (Bernet et al., 2019)) was subtracted from the difference between the Payerne MWR AOS dataset and the Bern MWR before the upgrade (in 2004). This relative bias was then removed from the Payerne MWR profile dataset prior to the 2005 intervention. For the 2009 homogenization, the difference between the Payerne MWR AOS dataset and MLS in 2010 was subtracted from the difference between the Payerne MWR AOS dataset and MLS in 2008. This relative bias was then removed from the Payerne MWR profile dataset prior to the 2009 intervention. These homogenizations are only possible if it is assumed the reference instruments (i.e. the Bern MWR and MLS) do not drift during the periods

considered. The Bern MWR dataset does not present any anomalies compared to other ground-based instruments in 2004 and 2007 (Bernet et al., 2019) and the MLS dataset does not present any anomalies compared to other satellite instruments between 2008 and 2010 (Hubert et al., 2016). Note that the mean drifts of 5–10%/decade measured between the MWRs and the satellites shown in Hubert et al. (2016) and Hubert (2019) are not representative of the drifts during the two year periods considered here.

Here again, the 2005 and 2009 technical issues affect the ozone profiles above 50 km differently depending on the LST. Figure 3c and d show the correction offset variation with LST for the 2005 and 2009 upgrades. Correction offsets have been evaluated by considering the 1h time bins. While a correction for 2005 is possible using the Bern MWR high time resolution dataset (Fig. 3c), in 2009 the lack of coincident measurements at high time resolution makes any LST-resolved correction very difficult. Coincident MLS measurements are available only twice a day (1 am and 1 pm overpasses) and the Bern MWR underwent an upgrade in 2009, meaning the stability of the dataset in term of measurement contribution during this particular period is uncertain (Fig. 3d).

A homogenised version of the 2000–2018 Payerne MWR dataset was thus made available for monthly means without any LST distinction above 50 km. For this study, we used the homogenised 2000–2018 timeseries of 1h LST-resolved monthly means for altitudes below 50 km, and the FFTS 2010–2018 timeseries of 2h LST-resolved monthly means for altitudes above 50 km. The deseasonalized ozone timeseries before and after the homogenization are plotted in Figure 4 for two representative layers in the middle stratosphere (4.18 hPa, 37 km) and in the low mesosphere (0.27 hPa, 57km).

4 Methods

4.1 Diurnal cycle calculation

The amplitude of the ozone diurnal cycle depends on altitude and varies seasonally. Above 0.59 hPa (50 km), the daytime ozone values are 15–25 % lower compared to the nighttime values, while at 5 hPa (35 km) afternoon values are up to 3% larger compared to nighttime values. The ozone diurnal cycle in the mesosphere has been intensively studied (Pallister and Tuck, 1983; Ricaud et al., 1996; Vaughan, 1984). The diurnal cycle of ozone in the stratosphere has been reported in Haefele et al. (2008), and the interannual variations of the ozone diurnal cycle described in Studer et al. (2014).

The diurnal ozone cycle is calculated relative to the nighttime value by:

$$O_{3,rel} = \frac{O_3 - O_{3,midnight}}{O_{3,midnight}} \quad (1)$$

where $O_{3,midnight}$ is an average of the ozone values from 22:00 to 02:00 LST at each pressure level.

4.2 Trend calculation

Trend estimates are obtained by fitting a multi-linear regression (MLR) function to the monthly mean ozone time series from each dataset. Trends are calculated for each pressure level independently and form a trend profile. We calculate average daytime

(10:00–14 LST) and nighttime (22:00-2:00 LST) trends as well as the trends for each hour of the day. The following MLR function is used:

$$O_3(t) = a + c_0\ t + \sum_{i=1}^{2} c_i \sin\left(\frac{2\pi i}{12} t\right) + \sum_{j=1}^{2} c_{j+2} \cos\left(\frac{2\pi j}{12} t\right) + c_5 \mathrm{SOL}(t) + c_6 \mathrm{QBO}_{10}(t)$$

$$+ c_7 \mathrm{QBO}_{30}(t) + c_8 \mathrm{ENSO}(t) + c_9 \mathrm{NAO}(t) + r(t) \quad (2)$$

The results are given as a % of the respective 2000–2010 mean. The proxies used represent sources of geophysical variability with known influence on stratospheric ozone, including the quasi-biennial oscillation (QBO at 30 hPa and 10 hPa), the 10.7 cm solar radio flux describing the 11-year solar cycle (SOL), the El Niño Southern Oscillation (ENSO), the North Atlantic Oscillation (NAO), and Fourier components representing the seasonal cycle (annual and semi-annual variations). t is in months, $r(t)$ is the residual~~noise~~, c_0 the linear component (the trend), and a the ordinate intercept of the regression line. The data sources for each proxy are provided in the data availability section at the end of this paper.

Stratospheric trends (below 50 km) are derived from data covering 2000 to 2018 while lower mesospheric trends (above 50 km) are derived from data covering 2010 to 2018. The solar cycle proxy has not been considered in the latter case because of the high probability of correlation with the linear slope when regressing timeseries shorter than one solar cycle.

All data points are considered with equal weights, and the uncertainty of the fit parameters is estimated from the regression residuals. Residual autocorrelations are removed using theCochrane-Orcutt transformation (Cochrane and Orcutt, 1949).

5 Results

5.1 Validation

Since the ozone profile time series used in this study is retrieved with an updated version of the OEM Arts/Qpack retrieval (see subsection 2.1), we carried out a new validation of the Payerne MWR dataset with ground-based and satellites ozone profile measurements.

5.1.1 Profiles of the mean relative differences

Individual Payerne MWR ozone profiles were compared with coincident satellite ozone profiles with a maximal temporal separation of 2h. The means of the relative differences between each satellite dataset and the Payerne MWR are plotted for the 25–65 km altitude range in Fig. 5a for daytime (10:00 LST–14:00 LST) and Fig. 5b for nighttime (22:00 LST–2:00 LST). The comparison with the HALOE sunset dataset is plotted on the daytime panel and the HALOE sunrise dataset on the nighttime panel, but these should be considered with caution given the low number of coincident measurements. The dotted lines represent the standard errors of the means.

The spread of the relative differences are as large as $\pm 12\%$. Similar differences (i.e. $\pm 5\%$ to $\pm 10\%$) are reported in studies comparing satellite datasets (Laeng et al., 2014; Rahpoe et al., 2015) and comparing ground-based and ~~satelite~~ satellite datasets (Hubert et al., 2016).

The mean relative difference of daytime profiles compared to MLS is approximately between -8 and +8% over the 30–65 km altitude range, while the relative difference compared to the HARMOZ datasets is between -10% and +10% over the 30–65 km altitude range. A systematic positive bias of the MIPAS, GBL, GOMOS, SCIAMACHY, HALOE and Bern MWR day and night datasets compared with the Payerne MWR is reported below 30 km. The larger relative difference compared to the HARMOZ datasets (when compared to the 5% difference with MLS) can be explained by the choice of the spatial coincidence criteria. The criteria for spatial coincidence (10° by 10°) may seem large but is necessary given the smaller number of coincidences. Reducing the spatial coincidence criterion from 10° to 6° in latitude (reducing the box from (1.95° E,41.82° N,11.95° E,51.82° N) to (1.95° E,43.82° N,11.95° E,49.82° N)) reduces the number of matches by more than 50%. However, the spatial distribution of matches is uneven, with a large number on the north and south borders of the box. This induces a larger bias, given the ozone gradient at these latitudes. The high density of the MLS measurements means that a reduced area can be used for the spatial coincidence criteria without degrading the statistics.

Below 48 km, the nighttime differences compared to MLS, GOMOS, and MIPAS are within ±5%. Above 50 km, the relative differences are as large as -7% compared to MLS and -15% compared to MIPAS and GOMOS. The Payerne MWR overestimates nighttime ozone at 55 km compared to all the satellite profiles except HALOE. The positive bias at night at 55 km was reported by Hocke et al. (2007) for a previous version of the Payerne retrieval. Rüfenacht and Kämpfer (2017) show that the emission signal of the secondary ozone layer can alter the nighttime ozone retrieval and thus the ozone values above 0.2 hPa can be overestimated. The a priori profiles and standard deviations used in the Payerne retrieval are identical for day- and nighttime conditions leading to the effects on the nighttime ozone profiles described in Rüfenacht and Kämpfer (2017), i.e. an overestimation of ozone at 55 km. Considering that the ozone secondary peak intensity is larger at night and that the width of the AVKs of the Payerne MWR dataset is on the order of 17 km in the lower mesosphere, the ozone information in the profile at 55 km is influenced by the ozone content at higher altitudes.

The ±10% agreement of the Payerne MWR with satellites assess the quality of the measurements considering the uncertainties of the respective instruments. The systematic 7% underestimation of ozone at 30 km is under investigation, while the nighttime 15% overestimation has been assigned to a mesospheric aliasing effect. The agreement between the two swiss MWRs is described in the next paragraph.

5.1.1.1 Relative difference compared to the Bern MWR

The mean relative difference between the Bern and Payerne MWRs lies between ±10% up to 40 km, increasing up to a maximum of -10 to -13% between 47–57 km .(Fig. 5). Since the measurement setups of the Bern and Payerne MWRs are very similar we would expect better agreement between the two instruments. However, the Payerne and Bern retrieval procedures differ in the calibration, in the a priori climatology used, as well as in the uncertainties used for the a priori and measurement covariance matrices, the spectroscopic parameters (pressure broadening), and in the temperature profiles used in the forward model. The measurement contribution and total error therefore slightly differ between the two MWRs. Based on a sensitivity study of the retrieval parameters of the Payerne MWR ozone profiles, the influence of the spectroscopic parameters is as high as ±7% at 50 km, while the influence of the forward model temperature profile is between ±2% at 50 km. Moreover, no period

weighting to account for anomalous measurements such as described in Bernet et al. (2019) has been applied to the Bern MWR dataset. Efforts are ongoing to harmonize the retrieval processes and it is future work to harmonize the two data processing chains to determine the sources for the differences.

5.1.1.2 Relative difference compared to SOCOL v3.0

The Payerne MWR and SOCOL climatological means agree within 15% at 50 km (Fig. 5). Above this level, the daytime values show differences of similar magnitude, but the nighttime differences are much larger, up to 40% at 0.2 hPa (60 km). The relative differences also ~~appears~~ appear to vary with season, with ozone values being closer in NH winter than in summer (not shown). The high time resolution of both the Payerne MWR and SOCOL simulations means that it is possible to derive ozone diurnal cycle profiles (Fig. 6). In the NH mid-latitudes, the daytime ozone levels vary with altitude from +4% at 4 hPa (36 km) to -25% at 0.2 hPa (60 km) with respect to nighttime values. The comparison of ozone diurnal cycles measured by the Payerne MWR and simulated by SOCOL v3.0 show good agreement, both with negative values during the day above 0.85 hPa, a minimum at sunrise, and a maximum in the afternoon, peaking at 12 hPa and 4 hPa respectively for Payerne MWR (Fig. 6a and b). The ~~desagreements~~ disagreements in amplitude and in height of transition from the lower mesospheric to the stratospheric diurnal cycle mode are slightly reduced when considering the AVK convolution of SOCOL v3.0 profiles to the Payerne MWR vertical resolution. This is due to the degradation of the model information vertical resolution (Fig. 6c) as described in (Studer et al., 2014).

SOCOL v3.0 overestimates the amplitude of the ozone diurnal cycle in the upper and middle (32–10 hPa) stratosphere and this could be related to the known overestimation of water vapor and upward transport in the model as well as to the positive temperature bias compared to ERA-40 (Stenke et al., 2013).

Despite a ~~poor agreement~~ modest agreement between the Payerne MWR and SOCOL v3.0 ozone content values, especially above 50 km, the good agreement between the Payerne MWR and SOCOL v3.0 ~~ozone values~~ diurnal variations in the 30 to 50 ~~km altitude range and moreover in their diurnal variations~~ km altitude range make it possible to consider the comparison of both datasets variation with LST. Nevertheless, the ~~desagreement~~ disagreement in the height of the diurnal cycle extremes has to be considered when comparing trends.

5.2 Multiple linear regression analysis

5.2.1 24-hour, daytime, and nighttime trends

Up to 50 km~~the 2000-2018~~, the 2000–2018 24-hour trend estimates are similar at the 95% confidence level to the 2000–2016 trend profiles of LOTUS NH ground-based datasets (Umkehr, LIDAR below 40 km) and a range of models as described in Petropavlovskikh et al. (2019) (Fig. 7). ~~Trends of~~ At 2 ~~%/dec at 2~~ hPa (43 km) ~~are~~ trend is with 2%/10y significantly positive. ~~For this study, we extended the time range by 2 years~~We tested the effect of the extended time span on the resuts. Effects on trends can be noticed below 30 km with a shift towards more positive values, while upper stratospheric trends do not vary significantly. At 50 km, the 24-hour average Payerne MWR trend is 2%/~~dec~~ 10y lower than the trends calculated from the

Dobson Umkehr, satellite, and model datasets used by Petropavlovskikh et al. (2019), which are all positive, but non-significant at that altitude.

Day- and nighttime trends for the 3 MWRs, MLS satellite and SOCOL CCM datasets, are plotted in Fig. 8. The lower panel shows 2000–2016 day- and nighttime trends up to 0.59 hPa (50 km). The upper panel concerns the 2010–2018 day- and nighttime trends in the low mesosphere. The focus here is the comparison of day- and nighttime trend profiles, being obvious that we cannot directly compare 2000–2016 with 2010–2018 trends. Similarly, the MLO MWR trends cannot be compared to the NH trends.

Day- and nighttime mid-stratospheric trends do not differ significantly at the 95% confidence level for the Payerne MWR, SOCOL, MLS satellite, or for the MLO MWR (lower panel of Fig. 8). The largest, but still not statistically significant, difference between day- and nighttime trends is measured at 45 km, with positive trend estimates ranging from 2 to 4%/~~dec~~ 10y for the Payerne MWR, and from 2 to 5%/~~dec~~ 10y for MLS. The statistically significant difference measured for the Bern MWR at 50 km is probably artificially produced by the 2009 homogenization which does not take into account the measurement contribution variation and/or a variation of the correction offset with LST. A similar behavior was observed for the Payerne MWR before the comprehensive homogenization of the AOS and FFTS datasets.

No significant differences between trends derived from day- and nighttime measuring instruments can therefore be attributed to a systematic measurement schedule difference between the instruments. As below 45 ~~km~~km, the diurnal cycle amplitude is minimal at sunrise and maximal in the afternoon, we do not expect any influence of the ozone diurnal cycle on the daytime and nighttime long-term trends at these altitudes. The potential influence of the diurnal cycle (ozone morning minimum and afternoon maximum) at these altitudes will be investigated by considering trends for each hour (see Sect.~~4.2.2~~ 5.2.2).

Day- and nighttime lower mesospheric trends do not differ significantly at 95% for the Payerne MWR, SOCOL, MLS satellite, or for the MLO MWR (upper panel of Fig. 8). The largest, but still not statistically significant, difference between day- and nighttime trends is measured at 57 km, with trend estimates ranging from 0 to 3%/~~dec~~ 10y for the Payerne MWR, and at 62 km, with trend estimates ranging from 0 to -2%/~~dec~~ 10y for MLS. At these altitudes too, no significant differences between trends derived from day- and nighttime measuring instruments can be attributed to a systematic measurement schedule difference, despite the fact that we expected an influence of the ozone diurnal cycle on the trend estimates in this altitude range. The day- and nighttime trends as measured by the Bern MWR are significantly negative in the lower mesosphere. We did not investigate the large negative nighttime trend estimates in this work but, as mentioned in Sect. ~~4.1~~5.1.1.1, intensive efforts are ongoing to homogenise the two swiss MWRs for the post-2010 period.

5.2.2 Payerne MWR ozone trends as a function of LST

In the stratosphere the ozone diurnal cycle ~~presents~~ shows a minimum at sunrise (∼12.5 hPa) and a maximum (∼4.16 hPa) in the afternoon (shown in Fig. 6). Long-term trends for each hour of the day were calculated using the method described in Sect.~~3.2~~ 4.2. This is only possible for the Payerne and Bern MWR datasets and for the SOCOL v3.0 simulations, which all have the necessary hourly time resolution.

In Fig. 9, one trend estimate in %/~~dec~~ 10y is plotted for each pressure level in the stratosphere and each hour of the day without any interpolation. Trend profiles in %/~~dec~~ 10y are shown as a function of LST, with hatches indicating values which are not significantly different from zero at the 95% confidence level. The Payerne MWR mid-stratospheric 2000–2018 trends are represented in Fig. 9a and Bern MWR trends in Fig. 9b. For each pressure level, the variations of ozone trends as a function of LST are small and the differences are not significant at the 95% confidence level. The largest, but still not statistically significant, difference is shown between 4 and 14 h LST at 40 km (Fig. 9c in red). Even when considering the altitude difference between the morning minimum and the afternoon maximum, the long-term ozone trends at the morning minimum (12.5 hPa, 8h LST, in blue) is similar to the long-term ozone trends at the afternoon maximum (4.16 hPa and 14h LST, in black) at the 95% confidence level.

5.2.3 SOCOL OH, NOx and temperature trends as a function of LST

Based on the correlation between ~~the~~ stratospheric O3 and ~~the~~ NOx, the active H and the Temperature long-term variations, and on the similarities of the ozone diurnal variation simulated by SOCOL and measured by the Payerne MWR, we investigate the variation of the NOx, OH and T trends with LST as an attempt to derive a correlation between ozone trend variation with LST and ozone-influencing substances trends variations with LST. We derive trends of simulated OH, NOx and T as a function of LST in the stratophere. We apply a similar MLR with proxies for the solar cycle, QBO at 30 hPa and 10 hPa, ENSO MEI and aerosols to monthly mean values for the 2000–2016 period.

Figure 10a shows the SOCOL OH linear trends as a function of LST. SOCOL shows a positive OH trend of 4%/~~dec~~ 10y during the day and a non significant trend of -2%/~~dec~~ 10y at night. No significant variation of daytime OH trend with LST is seen in the stratosphere. The OH impact on ozone chemistry in this altitude range is very limited when compared to NOx and Cl (Schanz, 2015). Active H influence increases from 0.3 hPa up, but is negligible at pressure levels lower than 2 hPa. During the night, OH disappears rather fast due to the absence of photolysis (OH production) and large OH reactivity (OH loss). The nighttime chemistry is mainly influenced by temperature, thus the nighttime ozone trend simulated by SOCOL should be related to the temperature trends (Fig. 10~~c~~b) and not to the OH trends.

Figure 10b shows the temperature trends as a function of LST. SOCOL shows a slightly negative trend of -1%/~~dec~~ 10y for both day- and nighttime between 30 km and 43 km. The negative trends are not significant out of this altitude range. Here again, no significant variation of temperature trend with LST is reported. We can only report a negative correlation between the negative temperature trend and the positive ozone trend independent of LST.

In the stratosphere, NOx variability plays a key role in ozone changes (Hendrick et al., 2012; Nedoluha et al., 2015a) with a maximum influence at 4 hPa. ~~A MLR with proxies for the solar cycle, the QBO at 30 and at 10~~ The same MLR was applied to monthly means of SOCOL simulated reactive NOx (NOx =NO+NO2) for the period 2000–2016 . Figure 10d shows the linear trends in simulated NOx as a function of LST. SOCOL shows a negative trend of -3%/~~dec~~ 10y in the morning and a statistically non-significant negative trend of -1%/~~dec~~ 10y in the afternoon. The variation with LST is again not significant at the 95% confidence level. The simulated NOx trends are agree with those reported by Hendrick et al. (2012), who shows negative trends of the NOx column for 24h-average datasets. Nedoluha et al. (2015b) demonstrated using HALOE (1991–2005) and

MLS (2004–2013) measurements that a significant decrease in ozone near 10 hPa in the tropics could be related to a spatially localized, but long-term increase in NOx. Although they also showed that the response of ozone to NOx chemistry varies strongly with time of day (Nedoluha et al., 2015a), with ozone destruction through the NOx cycle increasing from the morning to the afternoon (Schanz, 2015). Here we report negative trends in the morning and in the afternoon, but their difference is not significant at the 95% confidence level. However, when we consider just the global trends without any distinction by LST, we can see a similar negative correlation between the negative NOx trend and the positive O3 trend.

6 Conclusions

The 2000–2018 Payerne MWR dataset has been reprocessed and harmonized to ensure a constant measurement contribution to the ozone profiles and to take into account the effects of the three major technical upgrades (2001, 2005, and 2009). The dataset agrees now within $\pm 5\%$ with MLS over the 30 to 65 km altitude range and within $\pm 10\%$ of the HARMOZ satellite datasets over the 30 to 65 km altitude range. The Payerne MWR agrees within $\pm 15\%$ up to 50 km with the SOCOL v3.0 CCM. We report a 15% mean positive offset of the Payerne MWR datasets compared to other datasets at nighttime in the lower mesosphere. The overestimated nighttime ozone of the Payerne MWR is caused by an aliasing of the mesospheric nighttime ozone signal into the lower mesospheric ozone signal. Post-2000 long-term trends were calculated using MLR applied to the global Payerne MWR dataset and results agree well with other NH ground-based instrument trends published in Petropavlovskikh et al. (2019). Adding two more years to the dataset was shown to increase the trends below 30 km. A MLR was also applied to the high resolution data to assess whether significant trends could be detected in the ozone diurnal cycle. Neither stratospheric nor lower mesospheric ozone trends vary with LST significantly at the 95% confidence level. No significant long-term variation of the amplitude of the diurnal cycle is observed even if we consider the altitude difference of the ozone diurnal cycle minimum and maximum. Without any significant variation of the ozone trend with LST, no correlation is possible with the LST variation of temperature, OH and NO_x trends. We can only report a negative correlation between the negative NOx trend, the negative temperature trend and the positive ozone trend independent of LST in the stratosphere. From our quantification of the ozone trends as a function of LST we conclude, that systematic sampling differences between instruments cannot explain significant differences in trend estimates for the 2000–2018 period in the stratosphere and for the 2010-2018 period in the mesosphere.

Data availability. The most recent version of the Payerne MWR dataset will be available in the NDACC database at http://ftp.cpc.ncep.noaa.gov/ndacc/station/payerne/ames/mwave.

The Bern and Mauna Loa MWR datasets used for this study are available at http://ftp.cpc.ncep.noaa.gov/ndacc/station/bern/hdf/mwave and http://ftp.cpc.ncep.noaa.gov/ndacc/station/maunaloa/hdf/mwave.

The HARMOZ satellite datasets are available from ftp://ftp-ae.oma.be/esacci/ozone/Limb_Profiles/L2/HARMOZ_PRS.

The MLS ozone dataset is available from the NASA Goddard Space Flight Center Earth Sciences Data and Information Services Center (GES DISC) at http://disc.sci.gsfc.nasa.gov/Aura/data-holdings/MLS/index.shtml.

The sources for the proxy data used in the MLR are provided in Table 1.

Author contributions. EMB was responsible for the ground-based ozone measurements with the Payerne MWR, performed the data analysis and prepared the manuscript. AH and RR contributed to the interpretation of the results. LN provided the code for the trend calculations as function of LST. FT, WTB and EVR provided the SOCOL v3.0 dataset. KH, NK and LB were responsible for ground-based ozone measurements with the Bern MWR. IB and GN were responsible for ground-based ozone measurements with the MLO MWR. All co-authors contributed to the manuscript preparation.

Competing interests. The authors have no competing interests.

Acknowledgements. This work has been funded by MeteoSwiss within the Swiss Global Atmospheric Watch (GAW) program of the World Meteorological Organization. WTB was funded by SNSF projects 200020_163206 (SIMA) and 200020_182239 (POLE).

References

Ball, W. T., Alsing, J., Mortlock, D. J., Rozanov, E. V., Tummon, F., and Haigh, J. D.: Reconciling differences in stratospheric ozone composites, Atmospheric Chemistry and Physics, 17, 12 269–12 302, https://doi.org/10.5194/acp-17-12269-2017, 2017.

Ball, W. T., Alsing, J., Mortlock, D. J., Staehelin, J., Haigh, J. D., Peter, T., Tummon, F., Stübi, R., Stenke, A., Anderson, J., Bourassa, A., Davis, S. M., Degenstein, D., Frith, S., Froidevaux, L., Roth, C., Sofieva, V., Wang, R., Wild, J., Yu, P., Ziemke, J. R., and Rozanov, E. V.: Evidence for a continuous decline in lower stratospheric ozone offsetting ozone layer recovery, Atmospheric Chemistry and Physics, 18, 1379–1394, https://doi.org/10.5194/acp-18-1379-2018, 2018.

Ball, W. T., Alsing, J., Staehelin, J., Davis, S. M., Froidevaux, L., and Peter, T.: Stratospheric ozone trends for 1985-2018: sensitivity to recent large variability, Atmospheric Chemistry and Physics, 19, 12 731—12 748, https://doi.org/10.5194/acp-19-12731-2019, 2019.

Barnett, J. J., Houghton, J. T., and Pyle, J. A.: The temperature dependence of the ozone concentration near the stratopause, Quarterly Journal of the Royal Meteorological Society, 101, 245–257, https://doi.org/10.1002/qj.49710142808, 1975.

Bernet, L., von Clarmann, T., Godin-Beekmann, S., Ancellet, G., Maillard Barras, E., Stübi, R., Steinbrecht, W., Kämpfer, N., and Hocke, K.: Ground-based ozone profiles over central Europe: incorporating anomalous observations into the analysis of stratospheric ozone trends, Atmospheric Chemistry and Physics, 19, 4289–4309, https://doi.org/10.5194/acp-19-4289-2019, 2019.

Bertaux, J. L., Kyrölä, E., Fussen, D., Hauchecorne, A., Dalaudier, F., Sofieva, V., Tamminen, J., Vanhellemont, F., Fanton d'Andon, O., Barrot, G., Mangin, A., Blanot, L., Lebrun, J. C., Pérot, K., Fehr, T., Saavedra, L., Leppelmeier, G. W., and Fraisse, R.: Global ozone monitoring by occultation of stars: an overview of GOMOS measurements on ENVISAT, Atmospheric Chemistry and Physics, 10, 12 091–12 148, https://doi.org/10.5194/acp-10-12091-2010, 2010.

Bovensmann, H., Burrows, J. P., Buchwitz, M., Frerick, J., Noël, S., Rozanov, V. V., Chance, K. V., and Goede, A. P. H.: SCIAMACHY: Mission Objectives and Measurement Modes, Journal of the Atmospheric Sciences, 56, 127–150, https://doi.org/10.1175/1520-0469(1999)056<0127:SMOAMM>2.0.CO;2, 1999.

Buehler, S., Eriksson, P., Kuhn, T., von Engeln, A., and Verdes, C.: ARTS, the atmospheric radiative transfer simulator, Journal of Quantitative Spectroscopy and Radiative Transfer, 91, 65–93, https://doi.org/10.1016/j.jqsrt.2004.05.051, 2005.

Calisesi, Y.: Monitoring of stratospheric and mesospheric ozone with a ground-based microwave radiometer: data retrieval, analysis, and applications, Ph.D. thesis, Philosophisch- Naturwissenschaftliche Fakultät, Universität Bern, Bern, Switzerland, 77 pp., http://www.iap.unibe.ch/publications, 2000.

Chang, J. S., Brost, R. A., Isaksen, I. S. A., Madronich, S., Middleton, P., Stockwell, W. R., and Walcek, C. J.: A three-dimensional Eulerian acid deposition model: Physical concepts and formulation, Journal of Geophysical Research, 92, 14 681–14 700, https://doi.org/10.1029/JD092iD12p14681, 1987.

Chipperfield, M. P., Bekki, S., Dhomse, S., Neil, R. P., Hassler, B., Hossaini, R., Steinbrecht, W., Thiéblemont, R., and Weber, M.: Detecting recovery of the stratospheric ozone layer, Nature Publishing Group, 549, 211–218, https://doi.org/10.1038/nature23681, 2017.

Chubachi, S.: A special ozone observation at Syowa Station, Antarctica from February 1982 to January 1983, in: Atmospheric Ozone, pp. 285–289, https://doi.org/10.1007/978-94-009-5313-0_58, 1985.

Cochrane, D. and Orcutt, G. H.: Application of least squares regression to relationships containing auto-correlated error terms, J. Am. Stat. Assoc., 44, 32–61, 1949.

Connor, B. J., A., P., Tsou, J. J., and McCormick, P.: during measurements, Journal of Geophysical Research, 100, 9283–9291, 1995.

Craig, R. A. and Ohring, G.: The Temperature dependence of ozone radiational heating Rates in the vicinity of the mesopeak, Journal of Meteorology, 15, 59–62, https://doi.org/10.1175/1520-0469(1958)015<0059:TTDOOR>2.0.CO;2, 1958.

Damadeo, R. P., Zawodny, J. M., Remsberg, E. E., and Walker, K. A.: The Impact of Non-uniform Sampling on Stratospheric Ozone Trends Derived from Occultation Instruments, Atmospheric Chemistry and Physics, 18, 535—554, https://doi.org/10.5194/acp-18-535-2018, 2018.

Egorova, T. A., Rozanov, E. V., Zubov, V. A., and Karol, I. L.: Model for investigating ozone trends (MEZON), Izv. Atmos. Ocean. Phys., 39, 277–292, 2003.

Eriksson, P., Jiménez, C., and Buehler, S. A.: Qpack, a general tool for instrument simulation and retrieval work, Journal of Quantitative Spectroscopy and Radiative Transfer, 91, 47–64, https://doi.org/10.1016/j.jqsrt.2004.05.050, 2005.

Eyring, V., Cionni, I., Bodeker, G. E., Charlton-Perez, A. J., Kinnison, D. E., Scinocca, J. F., Waugh, D. W., Akiyoshi, H., Bekki, S., Chipperfield, M. P., Dameris, M., Dhomse, S., Frith, S. M., Garny, H., Gettelman, A., Kubin, A., Langematz, U., Mancini, E., Marchand, M., Nakamura, T., Oman, L. D., Pawson, S., Pitari, G., Plummer, D. A., Rozanov, E., Shepherd, T. G., Shibata, K., Tian, W., Braesicke, P., Hardiman, S. C., Lamarque, J. F., Morgenstern, O., Pyle, J. A., Smale, D., and Yamashita, Y.: Multi-model assessment of stratospheric ozone return dates and ozone recovery in CCMVal-2 models, Atmospheric Chemistry and Physics, 10, 9451–9472, https://doi.org/10.5194/acp-10-9451-2010, 2010.

Farman, J. C., Gardiner, B. G., and Shanklin, J. D.: Large losses of total ozone in Antartica reveal seasonal ClOx/NOx interaction, Nature, 315, 207–210, 1985.

Flury, T., Hocke, K., Haefele, A., Kämpfer, N., and Lehmann, R.: Ozone depletion, water vapor increase, and PSC generation at midlatitudes by the 2008 major stratospheric warming, Journal of Geophysical Research Atmospheres, 114, 1–14, https://doi.org/10.1029/2009JD011940, 2009.

Galytska, E., Rozanov, A., Chipperfield, M., Dhomse, S., Weber, M., Arosio, C., Feng, W., and Burrows, J.: Dynamically controlled ozone decline in the tropical mid-stratosphere observed by SCIAMACHY, Atmospheric Chemistry and Physics, 19, 767–783, https://doi.org/10.5194/acp-19-767-2019, 2019.

Giorgetta, M., Manzini, E., Roeckner, E., Esch, M., and Bengtsson, L.: Climatology and forcing of the quasi-biennial oscillation in the MAECHAM5 model, J. Climate, 19, 3882–3901, https://doi.org/10. 1175/JCLI3830.1, 2006.

Haefele, A., Hocke, K., Kämpfer, N., Keckhut, P., Marchand, M., Bekki, S., Morel, B., Egorova, T., and Rozanov, E.: Diurnal changes in middle atmospheric H2O and O3 : Observations in the Alpine region and climate models, Journal of Geophysical Research, 113, D17 303, https://doi.org/10.1029/2008JD009892, 2008.

Hendrick, F., Mahieu, E., Bodeker, G. E., Boersma, K. F., Chipperfield, M. P., De Mazière, M., De Smedt, I., Demoulin, P., Fayt, C., Hermans, C., Kreher, K., Lejeune, B., Pinardi, G., Servais, C., Stübi, R., Van Der A, R., Vernier, J. P., and Van Roozendael, M.: Analysis of stratospheric NO2 trends above Jungfraujoch using ground-based UV-visible, FTIR, and satellite nadir observations, Atmospheric Chemistry and Physics, 12, 8851–8864, https://doi.org/10.5194/acp-12-8851-2012, 2012.

Hocke, K., Kämpfer, N., Ruffieux, D., Froidevaux, L., Parrish, A., Boyd, I., von Clarmann, T., Steck, T., Timofeyev, Y. M., Polyakov, A. V., and Kyrölä, E.: Comparison and synergy of stratospheric ozone measurements by satellite limb sounders and the ground-based microwave radiometer SOMORA, Atmospheric Chemistry and Physics, 7, 4117–4131, https://doi.org/10.5194/acp-7-4117-2007, 2007.

Hubert, D.: The temporal and spatial homogeneity of ozone profile data records obtained by ozonesonde, lidar and microwave radiometer networks, in preparation, 2019.

Hubert, D., Lambert, J. C., Verhoelst, T., Granville, J., Keppens, A., Baray, J. L., Bourassa, A. E., Cortesi, U., Degenstein, D. A., Froidevaux, L., Godin-Beekmann, S., Hoppel, K. W., Johnson, B. J., Kyrölä, E., Leblanc, T., Lichtenberg, G., Marchand, M., McElroy, C. T., Murtagh, D., Nakane, H., Portafaix, T., Querel, R., Russell, J. M., Salvador, J., Smit, H. G., Stebel, K., Steinbrecht, W., Strawbridge, K. B., Stübi, R., Swart, D. P., Taha, G., Tarasick, D. W., Thompson, A. M., Urban, J., Van Gijsel, J. A., Van Malderen, R., Von Der Gathen, P., Walker, K. A., Wolfram, E., and Zawodny, J. M.: Ground-based assessment of the bias and long-term stability of 14 limb and occultation ozone profile data records, Atmospheric Measurement Techniques, 9, 2497–2534, https://doi.org/10.5194/amt-9-2497-2016, 2016.

Keating, G. M., Pitts, M. C., and Young, D. F.: Ozone reference models for the middle atmosphere, Advances in Space Research, 10, 317–355, https://doi.org/10.1016/0273-1177(90)90404-N, 1990.

Kyrölä, E., Tamminen, J., Sofieva, V., Bertaux, J. L., Hauchecorne, A., Dalaudier, F., Fussen, D., Vanhellemont, F., Fanton d'Andon, O., Barrot, G., Guirlet, M., Mangin, A., Blanot, L., Fehr, T., Saavedra de Miguel, L., and Fraisse, R.: Retrieval of atmospheric parameters from GOMOS data, Atmospheric Chemistry and Physics, 10, 11 881–11 903, https://doi.org/10.5194/acp-10-11881-2010, 2010.

Kyrölä, E., Laine, M., Sofieva, V., Tamminen, J., Pivrinta, S. M., Tukiainen, S., Zawodny, J., and Thomason, L.: Combined SAGE II-GOMOS ozone profile data set for 1984-2011 and trend analysis of the vertical distribution of ozone, Atmospheric Chemistry and Physics, 13, 10 645–10 658, https://doi.org/10.5194/acp-13-10645-2013, 2013.

Laeng, A., Grabowski, U., Von Clarmann, T., Stiller, G., Glatthor, N., Höpfner, M., Kellmann, S., Kiefer, M., Linden, A., Lossow, S., Sofieva, V., Petropavlovskikh, I., Hubert, D., Bathgate, T., Bernath, P., Boone, C. D., Clerbaux, C., Coheur, P., Damadeo, R., Degenstein, D., Frith, S., Froidevaux, L., Gille, J., Hoppel, K., Mchugh, M., Kasai, Y., Lumpe, J., Rahpoe, N., Toon, G., Sano, T., Suzuki, M., Tamminen, J., Urban, J., Walker, K., Weber, M., and Zawodny, J.: Validation of MIPAS IMK/IAA V5R-O3-224 ozone profiles, Atmospheric Measurement Techniques, 7, 3971–3987, https://doi.org/10.5194/amt-7-3971-2014, 2014.

Laeng, A., von Clarmann, T., Stiller, G., Dinelli, B. M., Dudhia, A., Raspollini, P., Glatthor, N., Grabowski, U., Sofieva, V., Froidevaux, L., Walker, K. A., and Zehner, C.: Merged ozone profiles from four MIPAS processors, Atmospheric Measurement Techniques, 10, 1511–1518, https://doi.org/10.5194/amt-10-1511-2017, 2017.

Lin, S. J. and Rood, R. B.: Multidimensional flux-form semi-Lagrangian transport schemes, Mon. Wea. Rev., 124, 2046–2070, 1996.

Livesey, N. J.: Earth Observing System (EOS) Aura Microwave Limb Sounder (MLS) Version 4.2x Level 2 data quality and description document, pp. 1–168, https://mls.jpl.nasa.gov/data/v4-2_data_quality_document.pdf, 2018.

Lossow, S., Khosrawi, F., Kiefer, M., Walker, K. A., Bertaux, J.-l., Blanot, L., Russell, J. M., Remsberg, E. E., Gille, J. C., Sugita, T., Sioris, C. E., Dinelli, B. M., Papandrea, E., Raspollini, P., Garcia-Comas, M., Stiller, G. P., von Clarmann, T., Dudhia, A., Read, W. G., Nedoluha, G. E., Damadeo, R. P., Zawodny, J. M., Weigel, K., Rozanov, A., Azam, F., Bramstedt, K., Noël, S., Burrows, J. P., Sagawa, H., Kasai, Y., Urban, J., Eriksson, P., Murtagh, D. P., Hervig, M. E., Högberg, C., Hurst, D. F., and Rosenlof, K. H.: The SPARC water vapour assessment II: Profile-to-profile comparisons of stratospheric and lower mesospheric water vapour data sets obtained from satellites, Atmospheric Measurement Techniques, 12, 2693—-2732, https://doi.org/10.5194/amt-12-2693-2019, 2019.

Mäder, J. A., Staehelin, J., Peter, T., Brunner, D., Rieder, H. E., and Stahel, W. A.: Evidence for the effectiveness of the Montreal Protocol to protect the ozone layer, Atmospheric Chemistry and Physics, 10, 12 161–12 171, https://doi.org/10.5194/acp-10-12161-2010, 2010.

Maillard Barras, E., Haefele, A., Stübi, R., and Ruffieux, D.: A method to derive the Site Atmospheric State Best Estimate (SASBE) of ozone profiles from radiosonde and passive microwave data, Atmospheric Measurement Techniques Discussions, 8, 3399–3422, https://doi.org/10.5194/amtd-8-3399-2015, 2015.

Marsh, D., Smith, A., and Noble, E.: Mesospheric ozone response to changes in water vapor, Journal of Geophysical Research: Atmospheres, 108, 4109, https://doi.org/10.1029/2002JD002705, 2003.

McPeters, R. D. and Labow, G. J.: Climatology 2011: An MLS and sonde derived ozone climatology for satellite retrieval algorithms, Journal of Geophysical Research Atmospheres, 117, https://doi.org/10.1029/2011JD017006, 2012.

Meul, S., Dameris, M., Langematz, U., Abalichin, J., Kerschbaumer, A., Kubin, A., and Oberländer-Hayn, S.: Impact of rising greenhouse gas concentrations on future tropical ozone and UV exposure, Geophysical Research Letters, 43, 2919–2927, https://doi.org/10.1002/2016GL067997, 2016.

Molina, M. J. and Rowland, F. S.: Stratospheric sink for chlorofluoromethanes: chlorine atom-catalysed destruction of ozone, Nature Geoscience, 249, 810–812, 1974.

Moreira, L., Hocke, K., Eckert, E., Von Clarmann, T., and Kämpfer, N.: Trend analysis of the 20-year time series of stratospheric ozone profiles observed by the GROMOS microwave radiometer at Bern, Atmospheric Chemistry and Physics, 15, 10 999–11 009, https://doi.org/10.5194/acp-15-10999-2015, 2015.

Nedoluha, G. E., Boyd, I. S., Parrish, A., Gomez, R. M., Allen, D. R., Froidevaux, L., Connor, B. J., and Querel, R. R.: Unusual stratospheric ozone anomalies observed in 22 years of measurements from Lauder, New Zealand, Atmospheric Chemistry and Physics, 15, 6817–6826, https://doi.org/10.5194/acp-15-6817-2015, 2015a.

Nedoluha, G. E., Siskind, D. E., Lambert, A., and Boone, C.: The decrease in mid-stratospheric tropical ozone since 1991, Atmospheric Chemistry and Physics, 15, 4215–4224, https://doi.org/10.5194/acp-15-4215-2015, 2015b.

Newnham, D. A., Clilverd, M. A., Kosch, M., Seppälä, A., and Verronen, P. T.: Simulation study for ground-based Ku-band microwave observations of ozone and hydroxyl in the polar middle atmosphere, Atmospheric Measurement Techniques, 12, 1375–1392, https://doi.org/10.5194/amt-12-1375-2019, 2019.

Pallister, R. C. and Tuck, A. F.: The diurnal variation of ozone in the upper stratosphere as a test of photochemical theory, Quarterly Journal of the Royal Meteorological Society, 109, 271–284, https://doi.org/10.1002/qj.49710946002, 1983.

Parrish, A., Connor, B. J., Tsou, J. J., McDermid, I. S., and Chu, W. P.: Ground-based microwave monitoring of stratospheric ozone, Journal of Geophysical Research, 97, 2541, https://doi.org/10.1029/91JD02914, 1992.

Parrish, A., Boyd, I. S., Nedoluha, G. E., Bhartia, P. K., Frith, S. M., Kramarova, N. A., Connor, B. J., Bodeker, G. E., Froidevaux, L., Shiotani, M., and Sakazaki, T.: Diurnal variations of stratospheric ozone measured by ground-based microwave remote sensing at the Mauna Loa NDACC site: Measurement validation and GEOSCCM model comparison, Atmospheric Chemistry and Physics, 14, 7255–7272, https://doi.org/10.5194/acp-14-7255-2014, 2014.

Parrish, A. D.: Millimeter-wave remote sensing of ozone and trace constituents in the stratosphere, Proc. IEEE, 82, 1915–1929, 1994.

Petropavlovskikh, I., Godin-Beekmann, S., Hubert, D., Damadeo, R. P., Hassler, B., Sofieva, V. F., Frith, S. M., and Tourpali, K.: SPARC/IOC/GAW report on Long-term Ozone Trends and Uncertainties in the Stratosphere, Report No. 9, GAW Report No. 241, WCRP-17/2018, https://doi.org/10.17874/f899e57a20b, 2019.

Poeschl, U., von Kuhlmann, R., Poisson, N., and Crutzen, P. J.: Development and intercomparison of condensed isoprene oxidation mechanisms for global atmospheric modeling, J. Atmos. Chem., 37, 29–52, https://doi.org/10.1023/A:1006391009798, 2000.

Rahpoe, N., Weber, M., Rozanov, A. V., Weigel, K., Bovensmann, H., Burrows, J. P., Laeng, A., Stiller, G., Von Clarmann, T., Kyrölä, E., Sofieva, V. F., Tamminen, J., Walker, K., Degenstein, D., Bourassa, A. E., Hargreaves, R., Bernath, P., Urban, J., and Murtagh, D. P.: Relative drifts and biases between six ozone limb satellite measurements from the last decade, Atmospheric Measurement Techniques, 8, 4369–4381, https://doi.org/10.5194/amt-8-4369-2015, 2015.

Revell, L. E., Tummon, F., Stenke, A., Sukhodolov, T., Coulon, A., Rozanov, E., Garny, H., Grewe, V., and Peter, T.: Drivers of the tropospheric ozone budget throughout the 21st century under the medium-high climate scenario RCP 6.0, Atmospheric Chemistry and Physics, 15, 5887–5902, https://doi.org/10.5194/acp-15-5887-2015, 2015.

Ricaud, P., de La Noë, J., Connor, B. J., Froidevaux, L., Waters, J. W., Harwood, R. S., MacKenzie, I. A., and Peckham, G. E.: Diurnal variability of mesospheric ozone as measured by the UARS microwave limb sounder instrument: Theoretical and ground-based validations, Journal of Geophysical Research: Atmospheres, 101, 10 077–10 089, https://doi.org/10.1029/95JD02841, 1996.

Rodgers, C. D.: Inverse Methods for Atmospheric Sounding - Theory and Practice, vol. 2 of *Series on Atmospheric Oceanic and Planetary Physics*, World Scientific Publishing Co. Pte. Ltd., Singapore, https://doi.org/10.1142/9789812813718, http://ebooks.worldscinet.com/ISBN/9789812813718/9789812813718.html, 2000.

Roeckner, E., Bäuml, G., Bonaventura, L., Brokopf, R., Esch, M., Giorgetta, M., Hagemann, S., Kirchner, I., Kornblueh, L., Manzini, E., Rhodin, A., Schlese, U., Schulzweida, U., and Tompkins, A.: The atmospheric general circulation model ECHAM 5.PART I: Model description, Tech. Rep., 349, 2003.

Rozanov, E., Calisto, M., Egorova, T., Peter, T., and Schmutz, W.: Influence of the precipitating energetic particles on atmospheric chemistry and climate, Surveys in Geophysics, 33, 483–501, https://doi.org/10.1007/s10712-012-9192-0, 2012.

Rüfenacht, R. and Kämpfer, N.: The importance of signals in the Doppler broadening range for middle-atmospheric microwave wind and ozone radiometry, Journal of Quantitative Spectroscopy and Radiative Transfer, 199, 77–88, https://doi.org/10.1016/j.jqsrt.2017.05.028, 2017.

Russell, J. M., Gordley, L. L., Park, J. H., Drayson, S. R., Hesketh, W. D., Cicerone, R. J., Tuck, A. F., Frederick, J. E., Harries, J. E., and Crutzen, P. J.: The Halogen Occultation Experiment, Journal of Geophysical Research, 98, 10 777–10 797, https://doi.org/10.1029/93JD00799, 1993.

Sander, S. P. e. a.: Chemical Kinetics and Photochemical Data for Use in Atmospheric Studies, Evaluation No. 17, Jet Propulsion Laboratory Publication, 10–6, http://jpldataeval.jpl.nasa.gov, 2011.

Schanz, A., Hocke, K., and Kämpfer, N.: Daily ozone cycle in the stratosphere: Global, regional and seasonal behaviour modelled with the Whole Atmosphere Community Climate Model, Atmospheric Chemistry and Physics, 14, 7645–7663, https://doi.org/10.5194/acp-14-7645-2014, 2014.

Schanz, A. U.: The diurnal variation in middle-atmospheric ozone : simulation and intercomparison, Ph.D. thesis, Philosophisch- Naturwissenschaftliche Fakultät, Universität Bern, Bern, Switzerland, 111 pp., http://www.iap.unibe.ch/publications, 2015.

Sofieva, V. F., Rahpoe, N., Tamminen, J., Kyrölä, E., Kalakoski, N., Weber, M., Rozanov, A., Von Savigny, C., Laeng, A., von Clarmann, T., Stiller, G., Lossow, S., Degenstein, D., Bourassa, A., Adams, C., Roth, C., Lloyd, N., Bernath, P., Hargreaves, R. J., Urban, J., Murtagh, D., Hauchecorne, A., Dalaudier, F., Van Roozendael, M., Kalb, N., and Zehner, C.: Harmonized dataset of ozone profiles from satellite limb and occultation measurements, Earth System Science Data, 5, 349–363, https://doi.org/10.5194/essd-5-349-2013, 2013.

Sofieva, V. F., Ialongo, I., Hakkarainen, J., Kyrölä, E., Tamminen, J., Laine, M., Hubert, D., Hauchecorne, A., Dalaudier, F., Bertaux, J. L., Fussen, D., Blanot, L., Barrot, G., and Dehn, A.: Improved GOMOS/Envisat ozone retrievals in the upper troposphere and the lower stratosphere, Atmospheric Measurement Techniques, 10, 231–246, https://doi.org/10.5194/amt-10-231-2017, 2017.

Solomon, S.: Stratospheric ozone depletion: A review of concepts and history, Reviews of Geophysics, 37, 275–316, https://doi.org/10.1029/1999RG900008, 1999.

Staehelin, J., Tummon, F., Revell, L., Stenke, A., and Peter, T.: Tropospheric Ozone at Northern Mid-Latitudes: Modeled and Measured Long-Term Changes, Atmosphere, 8, 163, https://doi.org/10.3390/atmos8090163, 2017.

Steinbrecht, W., Froidevaux, L., Fuller, R., Wang, R., Anderson, J., Roth, C., Bourassa, A., Degenstein, D., Damadeo, R., Zawodny, J., Frith, S., McPeters, R., Bhartia, P., Wild, J., Long, C., Davis, S., Rosenlof, K., Sofieva, V., Walker, K., Rahpoe, N., Rozanov, A., Weber, M., Laeng, A., von Clarmann, T., Stiller, G., Kramarova, N., Godin-Beekmann, S., Leblanc, T., Querel, R., Swart, D., Boyd, I., Hocke, K., Kämpfer, N., Maillard Barras, E., Moreira, L., Nedoluha, G., Vigouroux, C., Blumenstock, T., Schneider, M., García, O., Jones, N., Mahieu, E., Smale, D., Kotkamp, M., Robinson, J., Petropavlovskikh, I., Harris, N., Hassler, B., Hubert, D., and Tummon, F.: An update on ozone profile trends for the period 2000 to 2016, Atmospheric Chemistry and Physics, 17, 10 675–10 690, https://doi.org/10.5194/acp-17-10675-2017, 2017.

Stenke, A., Schraner, M., Rozanov, E., Egorova, T., Luo, B., and Peter, T.: The SOCOL version 3.0 chemistry-climate model: Description, evaluation, and implications from an advanced transport algorithm, Geoscientific Model Development, 6, 1407–1427, https://doi.org/10.5194/gmd-6-1407-2013, 2013.

Studer, S., Hocke, K., Schanz, A., Schmidt, H., and Kämpfer, N.: A climatology of the diurnal variations in stratospheric and mesospheric ozone over Bern, Switzerland, Atmospheric Chemistry and Physics, 14, 5905–5919, https://doi.org/10.5194/acp-14-5905-2014, 2014.

Sukhodolov, T., Rozanov, E., Shapiro, A. I., Anet, J., Cagnazzo, C., Peter, T., and Schmutz, W.: Evaluation of the ECHAM family radiation codes performance in the representation of the solar signal, Geosci. Model Dev., 7, 1–8, https://doi.org/0.5194/gmd-7-1-2014, 2014.

Tukiainen, S., Kyrölä, E., Tamminen, J., Kujanpää, J., and Blanot, L.: GOMOS bright limb ozone data set, Atmospheric Measurement Techniques, 8, 3107–3115, https://doi.org/10.5194/amt-8-3107-2015, 2015.

Vaughan, G.: Mesospheric ozone — theory and observation, Quarterly Journal of the Royal Meteorological Society, 110, 239–260, https://doi.org/10.1002/qj.49711046316, 1984.

Wang, W., Tian, W., Dhomse, S., Xie, F., Shu, J., and Austin, J.: Stratospheric ozone depletion from future nitrous oxide increases, Atmospheric Chemistry and Physics, 14, 12 967–12 982, https://doi.org/10.5194/acp-14-12967-2014, 2014.

Waters, J., Froidevaux, L., Harwood, R., Jarnot, R., Pickett, H., Read, W., Siegel, P., Cofield, R., Filipiak, M., Flower, D., Holden, J., Lau, G., Livesey, N., Manney, G., Pumphrey, H., Santee, M., Wu, D., Cuddy, D., Lay, R., Loo, M., Perun, V., Schwartz, M., Stek, P., Thurstans, R., Boyles, M., Chandra, K., Chavez, M., Gun-Shing Chen, Chudasama, B., Dodge, R., Fuller, R., Girard, M., Jiang, J., Yibo Jiang, Knosp, B., LaBelle, R., Lam, J., Lee, K., Miller, D., Oswald, J., Patel, N., Pukala, D., Quintero, O., Scaff, D., Van Snyder, W., Tope, M., Wagner, P., and Walch, M.: The Earth observing system microwave limb sounder (EOS MLS) on the aura Satellite, IEEE Transactions on Geoscience and Remote Sensing, 44, 1075–1092, https://doi.org/10.1109/TGRS.2006.873771, 2006.

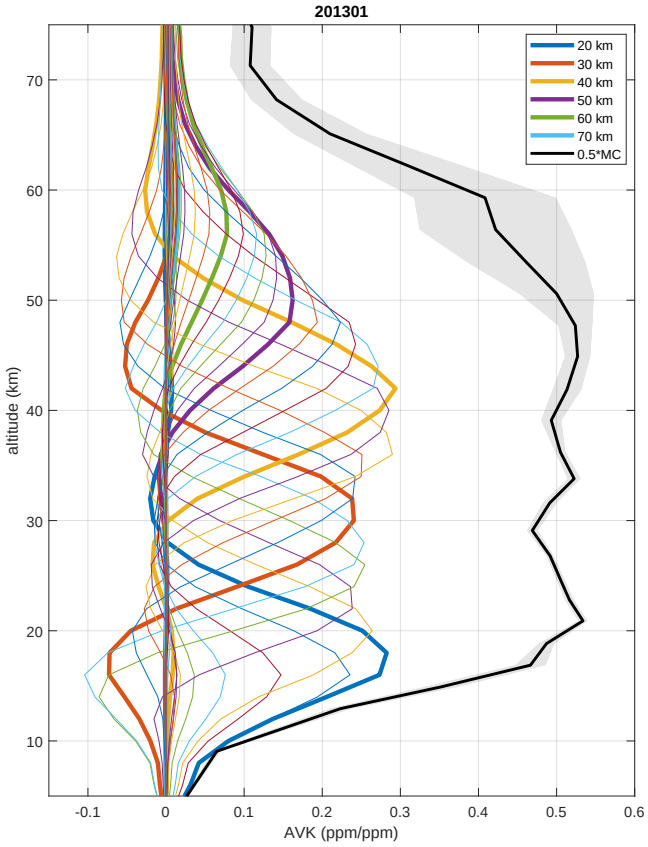

Figure 1. ~~Example~~ Mean values of Payerne MWR averaging kernels in ppm/ppm and measurement contribution ($\times 0.5$) for January, ~~2013~~2013. The shaded area represents the standard errors of the mean.

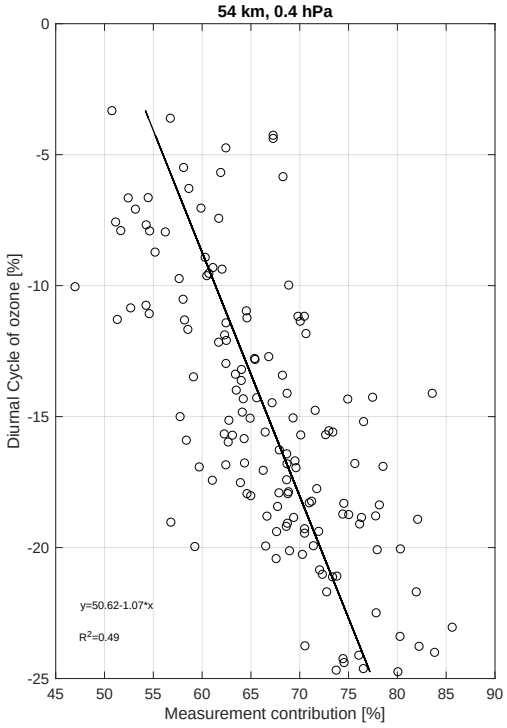

Figure 2. Ozone diurnal cycle amplitude (in % of midnight value) as a function of measurement contribution (in % of ozone content) for the lower mesosphere (0.4hPa).

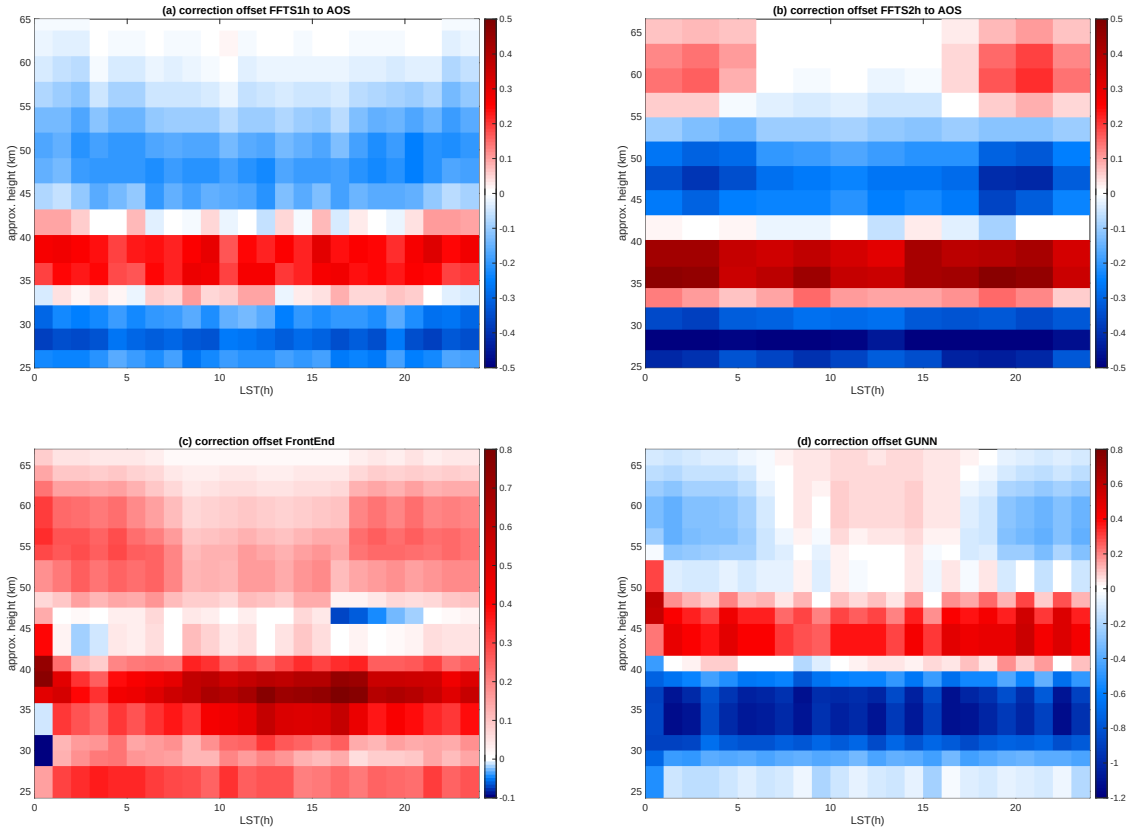

Figure 3. (a) and (b) Payerne MWR AOS setup vs FFT setup offset profiles in ppm as a function of LST, (c) correction offset for the front-end (in 2005) and (d) for the GUNN oscillator (in 2009) technical upgrades.

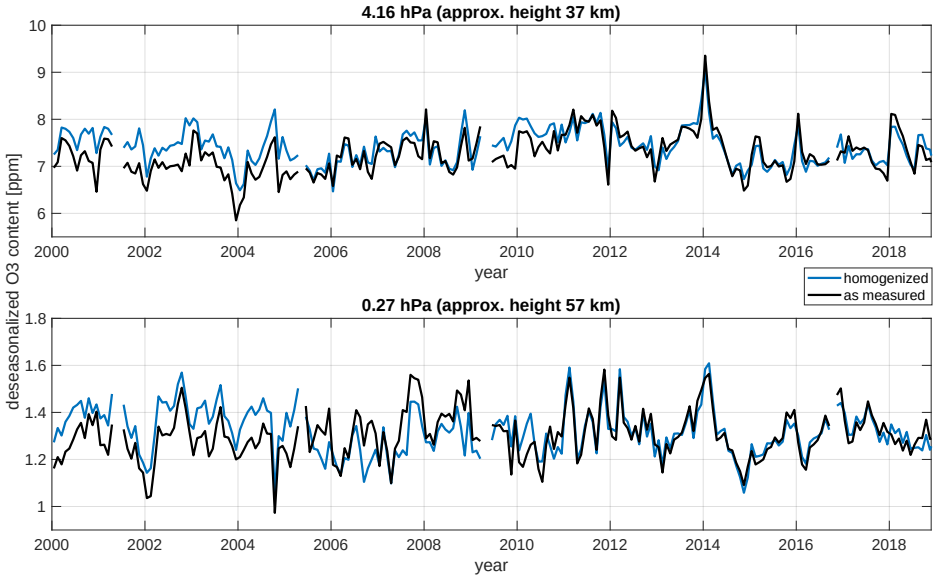

Figure 4. Deseasonalized ozone monthly means timeseries before (in black) and after (in blue) the homogenization for a representative layer in the middle stratosphere and in the low mesosphere.

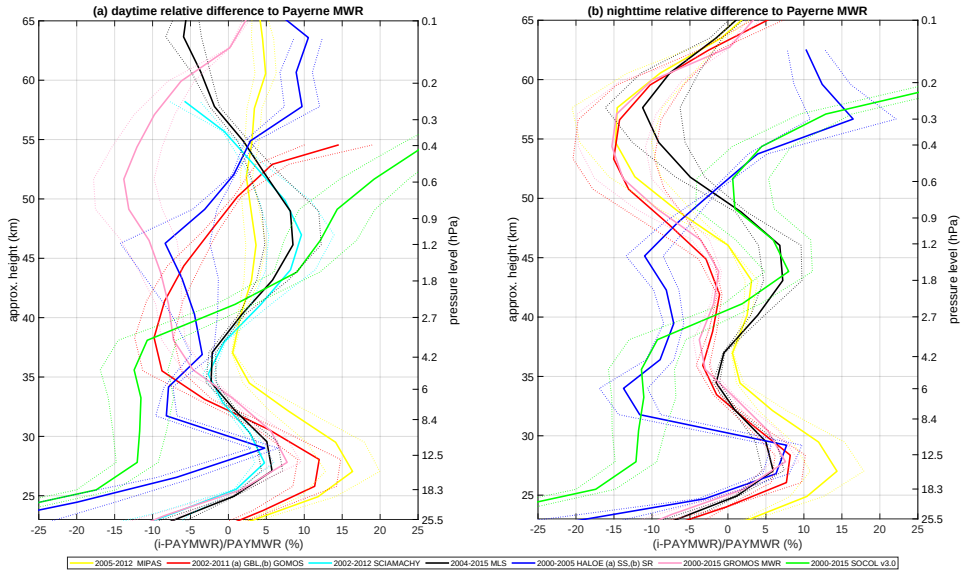

Figure 5. Payerne MWR bias vertical structure: mean of the relative difference between Payerne MWR and satellites MIPAS, MLS, GOMOS, GBL, SCIAMACHY, HALOE ((a) SS and (b) SR), and Bern MWR and SOCOL v3.0 CCM, for (a) daytime (10:00–14:00 LST) and (b) nighttime measurements (22:00–2:00 LST).

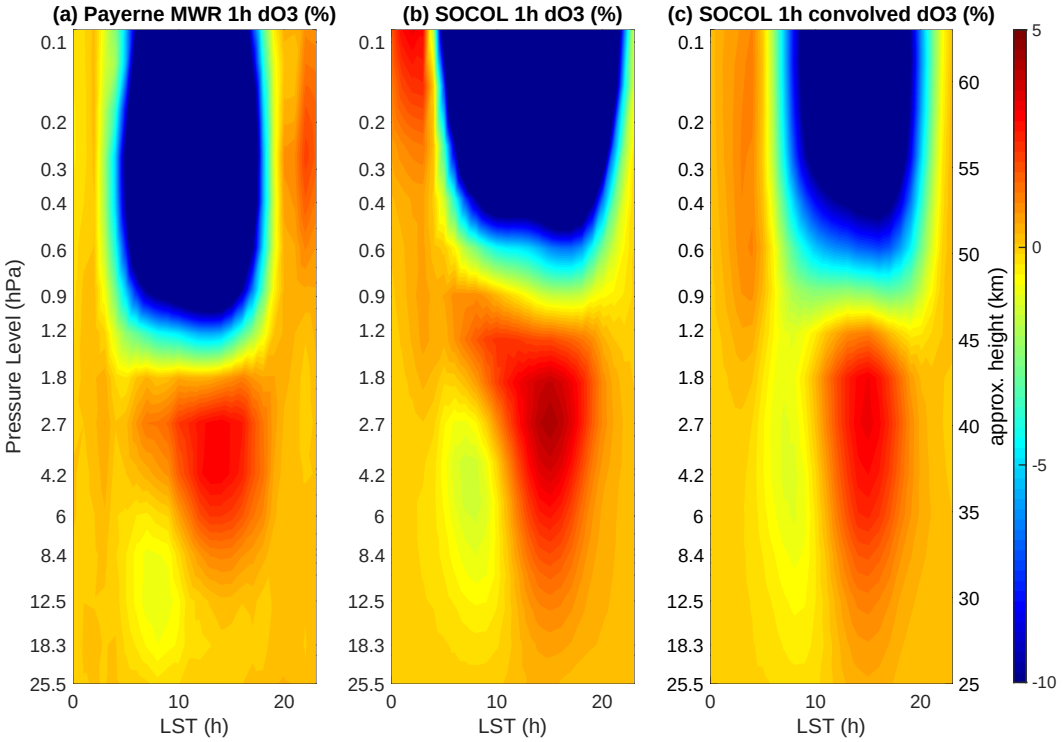

Figure 6. Annual mean O3 daily cycle measured by (a) Payerne MWR and (b)-(c) simulated by SOCOL v3.0 with a time step of 1h.

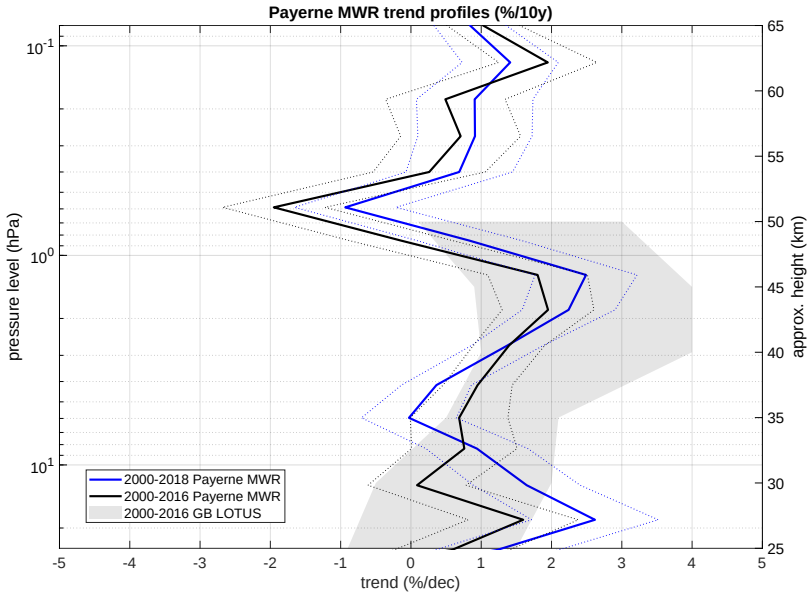

Figure 7. Payerne MWR O3 trend profiles for 2000–2016 time range in black and 2000–2018 time range in blue. The dotted lines show the 2σ uncertainties. The shaded area is the full range of LOTUS ~~GB 2000–2016~~ Ground-based 2000–2016 trend profiles.

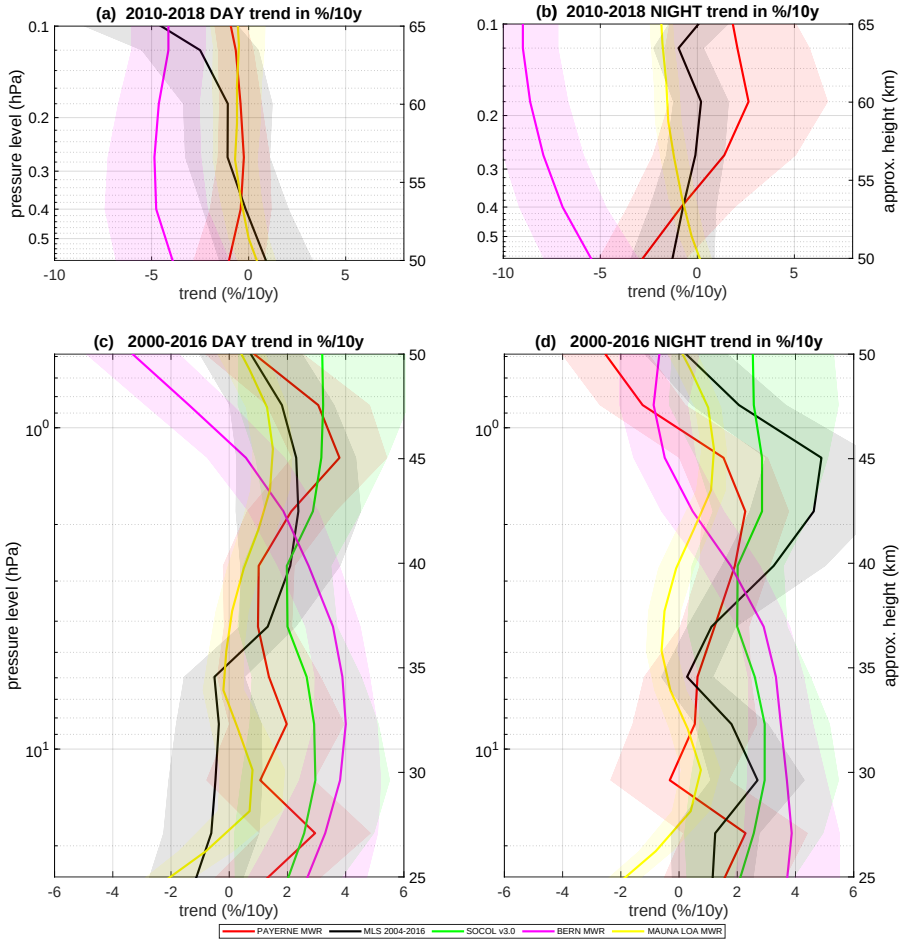

Figure 8. ~~2000–2018~~ 2000–2016 stratospheric (c and d) and 2010–2018 low-mesospheric (a and b) day- and nighttime trend profiles for Payerne MWR, MLS, SOCOL v3.0, Bern MWR, ~~2000–2016~~ 2000–2015 MLO MWR. The shaded areas show the 2 σ uncertainties.

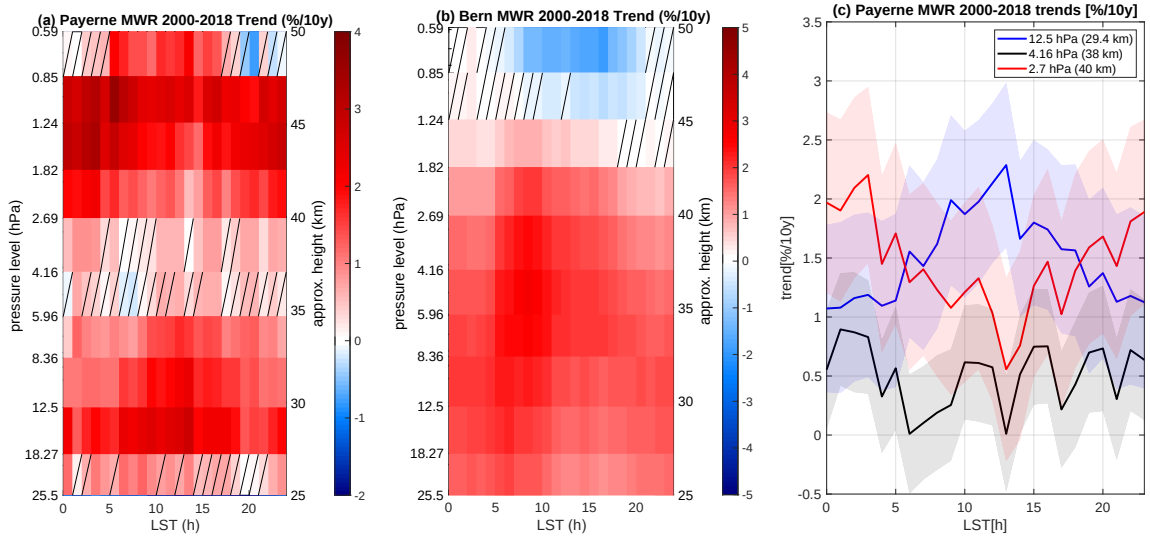

Figure 9. Long-term trends in %/~~dec~~ 10y vs LST for the ~~2000-2018~~ 2000–2018 period. Trend estimates non significantly different from zero at 95% are hatched.(a) Payerne MWR 1h time resolution dataset (b) Bern MWR 1h time resolution dataset (c) Payerne MWR O3 trends in %/~~dec~~ 10y at 2.7 hPa (red), at morning minimum (12.5 hPa, blue) and afternoon maximum (4.16 hPa, black) pressure levels vs LST.

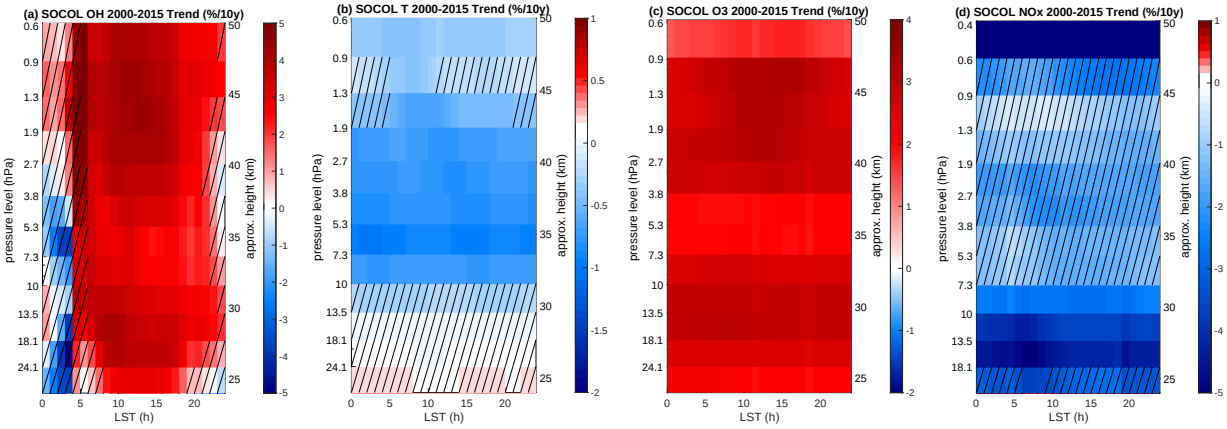

Figure 10. SOCOL v3.0 trends in %/~~dec~~ 10y vs LST (a) OH trends (b) T trends (c) O3 trends (d) NOx trends.

SOL	10.7 cm solar radio flux Penticton adjusted	http://www.spaceweather.gc.ca/solarflux/sx-5-mavg-eng.php
QBO10	Monthly mean zonal wind components at 10 hPa	http://www.geo.fu-berlin.de/met/ag/strat/produkte/qbo/index.html
QBO30	Monthly mean zonal wind components at 30 hPa	http://www.geo.fu-berlin.de/met/ag/strat/produkte/qbo/index.html
ENSO	Multivariate El Niño Southern Oscillation Index (MEI)	http://www.esrl.noaa.gov/psd/enso/mei/
NAO	North Atlantic Oscillations index	https://climatedataguide.ucar.edu/climate-data/hurrell-north-atlantic-oscillation-nao-index-station-based

Table 1. List of the explanatory variables used in the MLR model